Summer 2010

Activity Analysis of the Fragile X Mental Retardation Protein Isoforms 1, 2 and 3: Recombinant Bacterial Expression and Purification with Subsequent Quantitative Analysis of Binding to in vivo Target G quadruplex Forming Ribonucleaic Acids and Regulation of Translation

Timothy Lee Evans

ACTIVITY ANALYSIS OF THE FRAGILE X MENTAL RETARDATION PROTEIN ISOFORMS 1, 2 AND 3: RECOMBINANT BACTERIAL EXPRESSION AND PURIFICATION WITH SUBSEQUENT QUANTITATIVE ANALYSIS OF BINDING TO *IN VIVO* TARGET G QUADRUPLEX FORMING RIBONUCLEIC ACIDS AND REGULATION OF TRANSLATION

A Dissertation

Submitted to the Bayer School of

Natural and Environmental Sciences

Duquesne University

In partial fulfillment of the requirements for

the degree of Doctor of Philosophy

By

Timothy L. Evans

August 2010

ACTIVITY ANALYSIS OF THE FRAGILE X MENTAL RETARDATION PROTEIN ISOFORMS 1, 2 AND 3: RECOMBINANT BACTERIAL EXPRESSION AND PURIFICATION WITH SUBSEQUENT QUANTITATIVE ANALYSIS OF BINDING TO *IN VIVO* TARGET G-QUADRUPLEX FORMING RIBONUCLEIC ACIDS AND REGULATION OF TRANSLATION

By

Timothy L. Evans

Approved July 13, 2010

_____
Mihaela-Rita Mihailescu, Ph.D.
Associate Professor of Chemistry and Biochemistry
(Committee Chair)

_____
Mitchell E. Johnson, Ph.D.
Associate Professor of Chemistry and Biochemistry
(Committee Member)

_____
Charles T. Dameron, Ph.D.
Associate Professor of Chemistry
St. Francis University
(External Reviewer)

_____
David W. Seybert, Ph.D.
Dean, Bayer School of Natural and Environmental Sciences
Professor of Chemistry and Biochemistry
(Committee Member)

_____
Ralph A. Wheeler, Ph.D.
Chair, Department of Chemistry and Biochemistry
Professor of Chemistry and Biochemistry

ABSTRACT

ACTIVITY ANALYSIS OF THE FRAGILE X MENTAL RETARDATION PROTEIN ISOFORMS 1, 2 AND 3: RECOMBINANT BACTERIAL EXPRESSION AND PURIFICATION WITH SUBSEQUENT QUANTITATIVE ANALYSIS OF BINDING TO *IN VIVO* TARGET G-QUADRUPLEX FORMING RIBONUCLEIC ACIDS AND REGULATION OF TRANSLATION

By

Timothy L. Evans

August 2010

Dissertation supervised by Dr. Mihaela-Rita Mihailescu

The loss of expression of the fragile X mental retardation protein (FMRP) leads to fragile X syndrome. Fragile X syndrome is the most prevalent inheritable mental retardation. FMRP has two types of RNA binding domains, two K-homology domains and an arginine-glycine-glycine box domain, and is proposed to act as a translation regulator of specific mRNA. Despite extensive research, the mechanism by which FMRP loss leads to the fragile X syndrome remains unclear. Thus, there is high interest to produce sufficient quantities of pure recombinant FMRP for biochemical and biophysical studies of the protein function. However, the recombinant bacterial expression of FMRP has had limited success, and subsequent recombinant eukaryotic and *in vitro* systems may produce FMRP which is posttranslationally modified, as phosphorylation and arginine methylation have been shown to occur on FMRP. In this study, we have successfully

isolated the conditions for recombinant expression, purification and dialysis of full-length FMRP using *Escherichia coli*, with a high yield. The expression of FMRP using *E. coli* renders the protein devoid of the posttranslational modifications of phosphorylation and arginine methylation, allowing for the further study of the direct effects of these modifications individually and simultaneously. Additionally, FMRP has been shown to undergo alternative splicing, with one of the splicing sites in close proximity to the FMRP domain shown to be involved in binding G quadruplex mRNA with high affinity and specificity. We have analyzed how naturally occurring truncations in the FMRP sequence affect its RNA binding affinity, by applying the expression, purification and dialysis process to the second and third longest FMRP isoforms, followed by subsequent analysis of the G quadruplex mRNA binding properties by fluorescence spectroscopy. Our results show that as FMRP gets truncated by alternative splicing, its mRNA binding affinity increases. To test a model we proposed for FMRP translation regulation activity, we developed a luciferase reporter gene construct that contains the G quadruplex structure in the mRNA 5'-untranslated region. Using luminescence spectroscopy to analyze luciferase translation, we showed that low levels of full-length FMRP reduces luciferase translation, and as the concentration of full-length FMRP increases the luciferase translation increases.

DEDICATION

I dedicate this document, and everything it represents, to my wife and my father.

My wife, my Babydoll, Laura Evans, has provided so many things for me at such an unimaginable level that words could never contrive an accurate description. Your love, patience, sacrifice, and support have been invaluable and irreplaceable. I love you now and will love you forever at a level that far supersedes any level ever observed from one organism to another. Without question, God made you for me and I thank God daily for the day you randomly walked your beauty into my life.

My father, Dr. Morris Evans, has prepared me for my life, inside and outside of chemistry, exponentially better than any other individual ever could. You have been an irreplaceable source of patience, sacrifice, support, love, logic, experience, and expert advice. You are unquestionably the smartest and wisest person I will ever know and I am convinced that you can see the future. I thank God daily for the genes I inherited from you and I hope that someday I can be half the man you are.

I have fulfilled my goals of earning a Ph.D. and obtaining a position as a professor at a collegiate institution. Without the two of you, I would not have achieved my goals.

ACKNOWLEDGEMENT

First and foremost, I would like to acknowledge my advisor, Dr. Mihaela-Rita Mihailescu. You have nurtured my development into the scientist I have become. You enabled and allowed me to think independently during the course of my graduate work, fostering my critical thinking skills. You wealth of knowledge, inside and outside of chemistry, has been a critical asset for my development. The level of care and effort you extend to your students surpasses everything I have seen from any form that a teacher could take. I can thank you for virtually every good thing that will happen in my future and I would be lesser of a person if you had never been my advisor. I am also convinced that you can see the future.

I would like to acknowledge my initial advisor, Dr Charles T. Dameron. I have often referred to you as 'a walking encyclopedia of biochemistry,' and you have always lived up to that proclamation. You have been instrumental in my development as a scientist, particularly in the development of my laboratory skills and I will always think of you with great esteem.

I would like to acknowledge my committee member, Dr. Mitchell E. Johnson. You have been an excellent source of information and problem-solving throughout my graduate studies. Your questions and thoughts have taught me about alternate perspectives when analyzing a given situation, helping to develop my skills for thinking 'outside of the box.' Of particular importance to me is your personality, which allowed me to realize that professors are normal human beings. You are likely unaware that your stories have provided comic relief at critical times during my graduate studies.

I would like to acknowledge my committee member, Dr. David W. Seybert. You have been one of the main reasons I pushed myself during my graduate work. I am so impressed by your proven success and intelligence that I will likely always refer to you using the title of 'Dean.' I am very grateful for all of the time you took out of your immensely busy schedule as the Dean to tend to my needs.

I extend a special thank you to many of the people in my life at Duquesne University. Dr. Jeffry Madura, I wish you all the success you can imagine, you have been a role model for me in developing my skills for managing people, remaining unflappable, and critical thought. Ian Welsh, I will never forget the first time we met, the first and last time I asked you for help before 8 am, and all of the candy and laughs we have shared. I owe you immense gratitude for all of the help and effort you put forth on my behalf. Dan Bodnar, Dave Hardesty, and Lance Crosby, you gentlemen should have your official title at Duquesne University changed to 'lifesavers.' I have never witnessed a group of individuals that can come through in the clutch more than you gentlemen. I would like to extend a very special thank you to Courtney Sparacino-Watkins. We have been through an amazing and crazy journey to this point, and having you there with me has made it immensely better. I can only hope that you can say the same for me and you will always have a special place in my heart. I would also like to thank the original members from the laboratory of Dr. Charles T. Dameron: Dr. Kristina O. Pazehoski, Dr. Melinda A. Harrison, Dr. Tyler C. Collins, and Rachelle Palchesko. Your help, guidance, and friendship have been irreplaceable. I would like to thank Dr. Nathan Takas, Ryan and Sara Jonhson, and Matthew Purzycki for making my time as a graduate student to be considerably more tolerable. I would like to thank Amy Stroyne, Mary Jo Babinsack,

and Sandy Russell for their patience, support, hard work, and coming through in the clutch.

The laboratory group of Dr. Mihaela-Rita Mihailescu has been an invaluable source for my development. I would like to thank, in particular, Sumangala Shetty. The mental challenges you provided have been enjoyable and you have become a great friend. I have also been greatly touched and affected by Jessica Rabuck, Dr. Lakshmi Menon, Anna Blice-Baum, Valerie Schrott, Medhavi Bole, Kailey Ruszkowski, Julie Wong Chong, and Josh Lipay.

I would like to thank Duquesne University and the Department of Chemistry and Biochemistry. I would not be where I am without the opportunity and support provided.

I would like to acknowledge Slippery Rock University, and in particular Dr. Paul J. Birckbichler. You have been instrumental in preparing me for where I am today. You convinced me to become a biochemist, and I could not imagine a more enjoyable and rewarding career.

Finally, I would like to extend great thanks to my family. Mom, you have always pushed me to use my imagination, a tool that has proven pivotal in my field. I thank you for you love and prayers through thick and thin. Patti, I find it impossible for you to realize how much you mean to me. Sometimes I think about what it must have been like when you married my father, and along with it came three of the craziest boys known to man. I don't think you realized what you were getting yourself into when you married my father, but you have loved us boys as though we were your own, and I am forever grateful for this. It didn't take long for you to be 'family' to me, and I believe God made you for my father and for us boys, and without you there is no doubt that I would not be

where I am today. John, you have always been more than my brother, you have been my best friend. The bond we share is unlike anything that has ever existed between two brothers. I will never forget the day you were brought home from the hospital, and that this bond was formed virtually immediately. I will love you with all of my heart forever. Dave, you have helped me realize how fortunate I am. You make me laugh until I cry and I love you as much as Mom does, which is more than anyone else. Ray, you were a good man, and I hope I can be the man you were someday. I hope to see you again someday, in the meantime rest in peace in Heaven.

TABLE OF CONTENTS

Page

LIST OF TABLES

Page

LIST OF FIGURES

Page

LIST OF ABBREVIATIONS

Amp	ampicillin
2-AP	2-aminopurine
BSA	bovine serum albumin
CD	circular dichroism
CGG	cytosine-guanine-guanine
Chl	chloramphenicol
EDTA	ethylenediamine tetraacetic acid
FMR1	fragile X mental retardation gene
FMRP	fragile X mental retardation protein
FXS	fragile X syndrome
ISO1	FMRP isoform 1
ISO2	FMRP isoform 2
ISO3	FMRP isoform 3
KH	K-homology domain
LB	luria-bertani
luc	luciferase gene
MALDI-TOF-MS	matrix-assisted laser desorption/ionization-time of flight-mass spectrometry
MAP1B	microtubule associated protein 1B
MAP1B_19AP	fragment of microtubule associated protein 1B mRNA that forms a G quadruplex and contains 2-aminopurine at position 19

mGluR5	metabotropic glutamate receptor 5
mRNA	messenger RNA
mRNP	messenger ribonucleoprotein complex
NES	nuclear export sequence
NLS	nuclear localization sequence
PRMT	protein arginine methyltransferase
RGG box	arginine-glycine-glycine box domain
RNA	ribonucleic acid
RRL	rabbit reticulocyte lysates
S3F-sh	fragment of semaphorin 3F mRNA that forms a G quadruplex
S3F-sh_8AP	semaphorin 3F mRNA containing 2-aminopurine at position 8
SDS-PAGE	sodium dodecyl sulfate-polyacrylamide gel electrophoresis
UTR	untranslated region

CHAPTER 1: INTRODUCTION

1.1 Fragile X Syndrome: Background and History

The connection between sex-linked inheritance and mental retardation was first shown in 1943 and, in 1969, patients afflicted with this disorder were shown to have an abnormal X chromosome structure which was designated as the fragile X chromosome [1, 2]. In 1991, the fragile X mental retardation gene (*FMR1*) was discovered and it was shown that a gene mutation, specifically an unstable trinucleotide repeat expansion, occurred in patients diagnosed with fragile X syndrome (FXS) [3]. FXS is the most prevalent inheritable mental retardation in humans, affecting approximately one in 4000 males and one in 8000 females [4]. Patients diagnosed with FXS exhibit phenotypic IQ scores of 20 to 60, hyperactivity, avoidance of eye contact, and about 30% also have autism [5]. In addition to the cognitive defects, FXS patients have increased head-size, elongated face, protruding ears, and males experience macro-orchidism.

1.2 Fragile X Syndrome: Molecular Diagnosis and Gene Mutation

The FXS phenotype is caused by the loss of expression of the fragile X mental retardation protein (FMRP) [6-8], whose transcriptional silencing is caused by an expansion of greater than 200 cytosine-guanine-guanine (CGG) repeats in the 5'-untranslated region (UTR) of the *FMR1* gene [5, 7, 8]. The cytosines of this region of CGG repeats, along with an upstream CpG island, become hyper-methylated. The combined effects of the trinucleotide repeat expansion and hyper-methylation events are thought to directly block binding of transcription factors and/or to cause chromatin

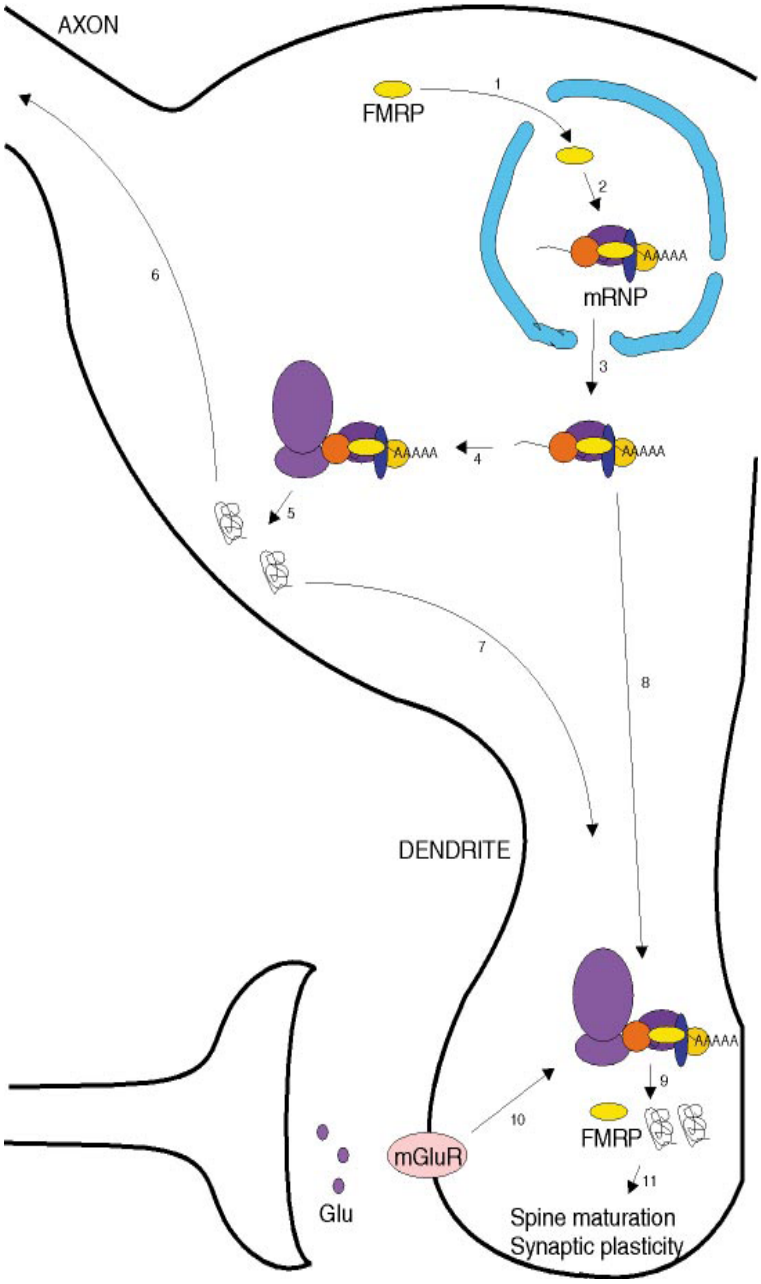

Figure 1. Model of FMRP function in the neuron. FMRP is transported into the nucleus of neurons via its nuclear localization signal (1). Once in the nucleus FMRP associates with cellular mRNAs as well as a number of proteins to form a large ribonucleoprotein complex (mRNP) (2) that is subsequently transported out of the nucleus via the nuclear export signal of FMRP (3). Once in the cytoplasm the FMRP mRNP can either associate with ribosomes in the cell body (4) producing proteins (5) that can be transported into the axon (6) or dendrites (7), or the FMRP mRNP can itself be transported into the dendrites (8) and associate with ribosomes to produce proteins in response to metabotropic glutamate receptor (mGluR) activation (10). Both the local translation of proteins in the dendrite and transport of proteins from the cell body mediate synaptic plasticity and spine maturation (11). Adapted from [8].

condensation, which in turn blocks the binding of transcription factors. Since the discovery that the FMRP transcription loss leads to FXS, much effort has been put forth in the study of FMRP; however, the function of the protein, the role it plays in the brain, and how its loss leads to mental retardation have not been fully elucidated.

1.3 Fragile X Mental Retardation Protein

FMRP is found primarily in the neurons and testes and it is thought that FMRP acts a regulator of gene expression at the level of translation. The proposed role of FMRP is to bind specific target messenger RNAs (mRNAs), transport those mRNAs throughout the cell, and regulate their translation in response to synaptic input (Fig 1) [8].

FMRP contains two different RNA binding domains, the arginine-glycine-glycine box (RGG box) domain and two K-homology (KH) domains, KH1 and KH2 (Fig 2A) [8]. FMRP also has a nuclear localization signal (NLS), as well as a nuclear export signal (NES) [8]. Additionally, FMRP has been shown to undergo the posttranslational modifications of phosphorylation and arginine methylation [9, 10].

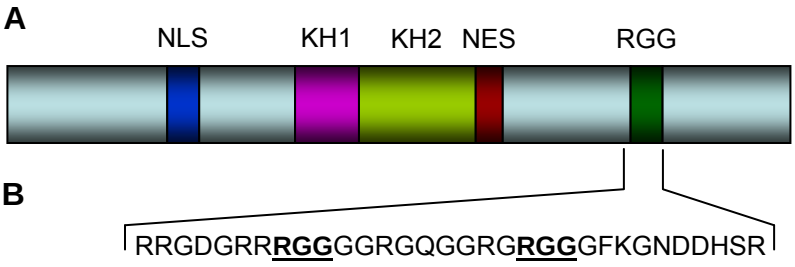

Figure 2. (A) Schematic of full-length FMRP showing the nuclear localization signal (NLS) in blue, the K-homology domains (KH1, KH2) in pink and light green respectively, the nuclear export signal (NES) in red, and the RGG box domain (RGG) in green. **(B)** Sequence of the FMRP RGG box domain showing the RGG repeats underlined and bolded. Adapted from [4].

The presence of both the NLS and the NES led to the proposal that, through these localization signals, FMRP shuttles between the nucleus and cytoplasm, hence, acting to transport a subset of mRNAs from the nucleus to the distant sites in the cell (Fig 1) [11]. FMRP has indeed been detected in both the cytoplasm and, in smaller quantities, the nucleus [11-13]. It has been proposed that nascent FMRP is part of polyribosomal complexes in the cytoplasm and that normal dissociation from the polyribosomes along with the presence of the NLS enables FMRP to be transported into the nucleus. Then, in response to growth stimuli, FMRP is transported into the nucleus where it binds its target mRNAs. The subsequent transport back to the cytoplasm is exportin 1-dependent and the FMRP-mRNA complex once again associates with ribosomes.

The RGG box, found in select RNA binding proteins, was first described in 1991 (Fig 2B) [14]. There is no consensus sequence for this domain and the RGG box was originally defined as having two or more RGG repeats interspersed with other, particularly aromatic, residues. More recent bioinformatic analysis with parameters of two or three RGG repeats, having five to nine residues separating the repeats, identified 44 human proteins that contain RGG boxes [15]. This indicates both the variability of the RGG box domain sequences and, based on the number of proteins found, the biological relevance of the RGG box. Proteins containing the RGG box domain also typically contain other RNA binding domains, for example FMRP contains two KH domains and the RGG box domain. One possible explanation is that the mRNA targets of RGG box containing proteins vary, thus, the RGG box could act in tandem or synergistically with the other RNA binding domains during the mRNA binding process. Alternately, the

multiple different RNA binding domains contained within a given protein could act independent of one another and target different RNAs.

Biochemical studies have shown that the RGG box of FMRP targets and binds certain guanine-rich mRNA sequences that fold into the G quadruplex secondary structure (Fig 3) [4, 6, 16, 17]. Formed from four guanine residues, a G quartet has a planar conformation stabilized by Hoogsteen base pairing and a central K^+ ion (Fig 3A) [4, 18]. Several planar G quartets stack to form G quadruplex structures (Fig 3B). It is thought that the RGG box domain is dynamic and unstructured, becoming structured upon binding of G quadruplex mRNA.

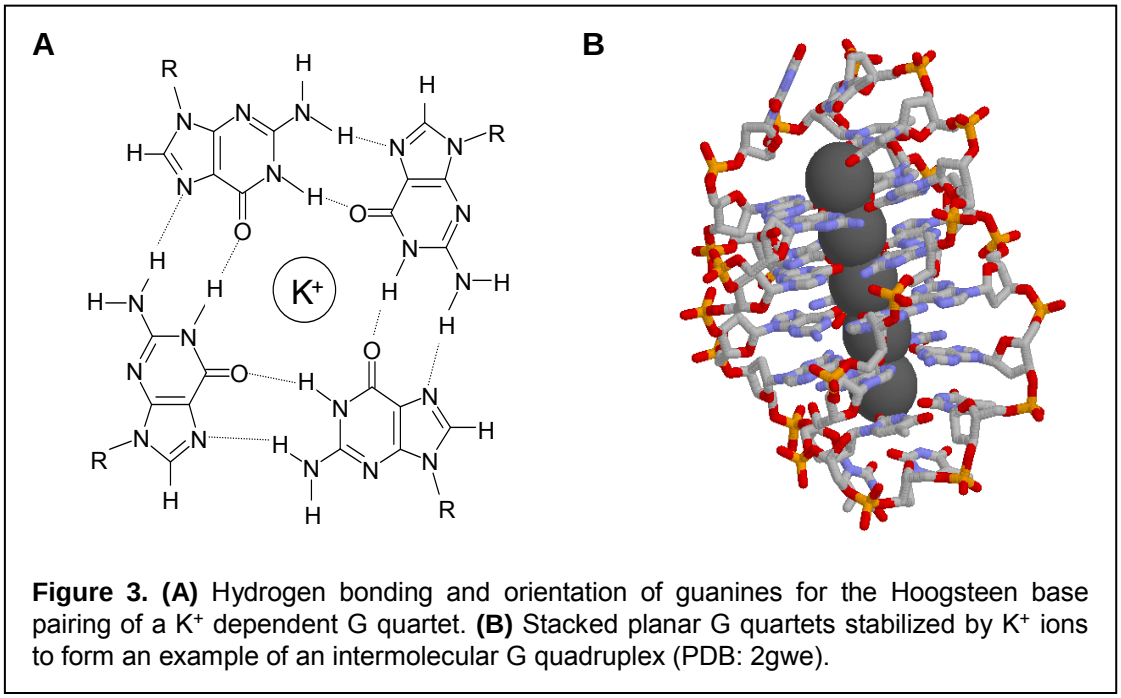

Figure 3. (A) Hydrogen bonding and orientation of guanines for the Hoogsteen base pairing of a K^+ dependent G quartet. **(B)** Stacked planar G quartets stabilized by K^+ ions to form an example of an intermolecular G quadruplex (PDB: 2gwe).

In addition to the RGG box, FMRP possesses two separate KH domains (Fig 2A). The KH domain, first identified and named from the human heterogeneous nuclear ribonucleoprotein K, consists of approximately 70 residues, is involved in a myriad of

processes such as mRNA splicing or transcriptional regulation, and is found in a diverse variety of proteins in archaea, prokaryotes and eukaryotes [19]. The typical function of the KH domain is RNA and single-stranded DNA recognition, and the domain is typically found in multiple copies within the same protein. It has been shown that FMRP uses its KH2 domain to bind to RNAs which form the kissing-loop secondary structure [20]. The kissing-loop structure is a stable complex formed by Watson-Crick base-pairing between the loops of two RNA hairpins. The kissing-loop structure is highly dependent on divalent cations and is found in prokaryotes, eukaryotes and viruses [21].

Recent studies have revealed a novel mechanism to regulate gene expression at the level of translation, which is proposed to involve the G quadruplex mRNA secondary structure (Fig 3B) [22]. However, the full extent of the mRNA G quadruplex biological activity is not well understood, and the role it plays in translation regulation, or any other processes, have not been fully elucidated. Biophysical studies have shown that both DNA and RNA containing specific guanine-rich sequences can fold into G quadruplexes. DNA G quadruplexes became of special interest in the past decade as it was discovered that they are dispersed in eukaryotic genomes, being abundant in regions of biological significance such as the telomeres and the promoters of many important genes [23]. There are, however, fewer examples of RNA G quadruplexes, which have been proposed to be involved in transcription regulation, translation regulation, and in interacting with prion proteins [24]. It is known that the genetic information governing translation is localized mainly to the 5'- and 3'-UTR of mRNA and that it may involve both the sequence and secondary structure of these non-protein coding regions [22]. Bioinformatic analysis has found that 2334 and 3530 G quadruplexes could potentially

exist in the 5'- and 3'-UTRs, respectively, of human mRNA transcripts from known protein-coding genes. Furthermore, the role of the G quadruplex mRNA secondary structure as a mode of posttranscriptional regulation has been confirmed by showing that the individual introduction of known G quadruplexes from the 5'-UTRs of two different mRNAs into the mRNA 5'-UTR of a reporter gene which resulted in the translation inhibition of the reporter gene [25, 26]. The mRNA G quadruplex structure shows promise as a mechanism the cell uses to control gene expression at the level of translation, and the fact that it is recognized and bound by the RGG box domain of FMRP is of high interest. Additionally, a patient recently diagnosed with FXS showed normal levels of FMRP (Dr. Bassem Hassan, Katholieke Universiteit Leuven, unpublished data). Genetic analysis showed a frameshift mutation that occurs between the RGG repeats of the RGG box domain, thereby abolishing over half the RGG box domain and eliminating the second RGG repeat, truncating the C-terminus of FMRP, and changing the identity of the residues that remained after the mutation site. The elimination of a functional RGG box domain for this patient, which expresses normal levels of mutated FMRP, illustrates the importance of this domain for the function of FMRP.

The mRNA product of the *FMR1* gene has been shown the undergo alternative splicing that involves exons 12 and 14 and the choice of acceptor sites in exons 15 and 17 [27-30]. These splicing patterns could potentially form 20 different isoforms, however so far only five different isoforms have been detected in various tissues (Fig 4) [27, 28, 31, 32]. Neither the relative levels of expression, nor the prevalent distributions of the various exon splicing products are known [33]. This study focuses on the three longest

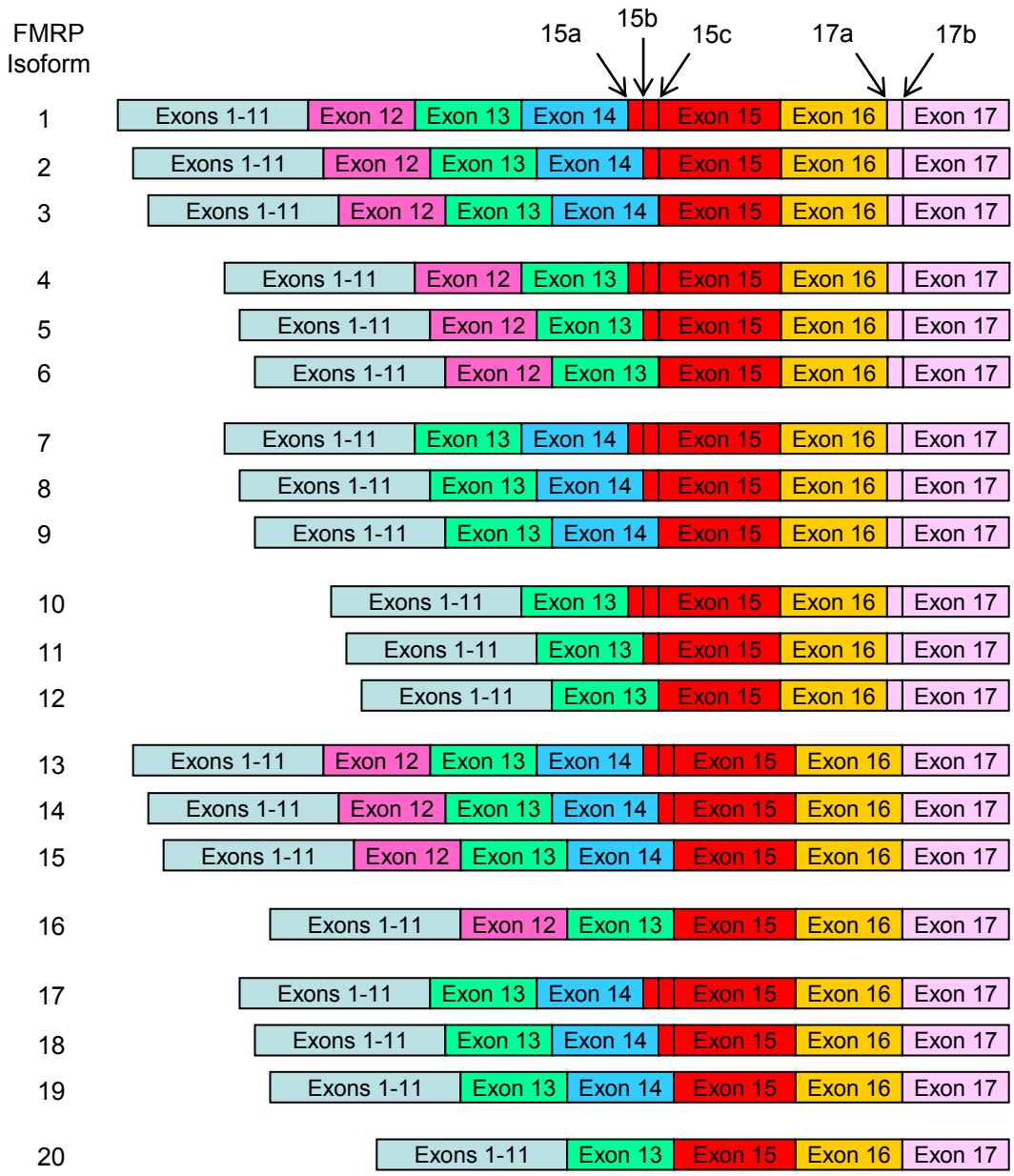

Figure 4. Schematic of the 20 possible FMRP isoforms resultant from alternative splicing of the FMR1 mRNA. The three exon 15 splice acceptor sites are 15a, 15b and 15c. The two exon 17 splice acceptor sites are 17a and 17b. The FMRP isoforms expressed in this study, ISO1, ISO2 and ISO3, vary based on the three exon 15 acceptor sites. Specifically, ISO1 utilizes splice acceptor site 15a, while ISO2 and ISO3 utilize sites 15b and 15c, respectively. ISO4, ISO5 and ISO6 are identical to ISO1, ISO2 and ISO3, respectively, but lack exon 14. ISO7, ISO8 and ISO9 are identical to ISO1, ISO2 and ISO3, respectively, but lack exon 12. ISO10, ISO11 and ISO12 are identical to ISO1, ISO2 and ISO3, respectively, but lack both exons 12 and 14. ISO13, ISO14 and ISO15 are identical to ISO1, ISO2 and ISO3, respectively, except utilize splice acceptor site 17b. ISO16 is identical to ISO15 but lacks exon 14. ISO17, ISO18 and ISO19 are identical to ISO7, ISO8 and ISO9, respectively, except utilize splice acceptor site 17b. ISO20 is identical to ISO15 but lacks exons 12 and 14. Adapted from [13].

FMRP protein products, isoform 1, 2 and 3 (ISO1, ISO2 and ISO3 respectively) (Fig 5). The immature *FMR1* transcript contains 17 exons, and the ISO2 and ISO3 products result from the three alternate splice acceptor sites at exon 15. ISO1, representing the longest expressed FMRP isoform, is truncated by 13 residues to form ISO2 and another 12 residues to form ISO3. All three FMRP isoforms maintain the NLS, KH1, KH2, NES and RGG box domains. The splice formation of ISO2 and ISO3 does result in the loss of the residues shown to be posttranslationally phosphorylated. The interest in these three FMRP isoforms stems, in part, from the fact that these truncations are in upstream close proximity to the RGG box. As stated previously, it is thought that the region surrounding and including the RGG box is predominately unstructured, hence the intent to elucidate the effects of these naturally occurring truncations in this dynamic region on the FMRP RGG box ability to bind G quadruplex mRNAs.

Mammalian FMRP was found to be phosphorylated in a region located N-terminal and in the close proximity, to the RGG box domain (Fig 5) [9, 34]. It has been shown that unphosphorylated FMRP associates with actively translating polyribosomes, while phosphorylated FMRP associates with stalled polyribosomes, suggesting that this posttranslational modification modulates the FMRP translation regulator function [35]. The two enzymes implicated in the phosphorylation and dephosphorylation of FMRP were identified as the ribosomal protein S6 kinase and the protein phosphatase 2A, respectively [36, 37]. It has been proposed that FMRP phosphorylation is coupled to translation repression, whereas FMRP dephosphorylation signals the release of the target mRNAs for translation [36-38]. In addition, it has been proposed that the phosphorylation state of FMRP determines its inclusion with the microRNA pathway by

regulating its association with Dicer and Dicer-containing complexes [34]. It is, however, unclear if these phosphorylation and dephosphorylation events regulate the FMRP translation regulation activity by affecting its binding properties for G quadruplex forming mRNA, or its interactions with other protein partners.

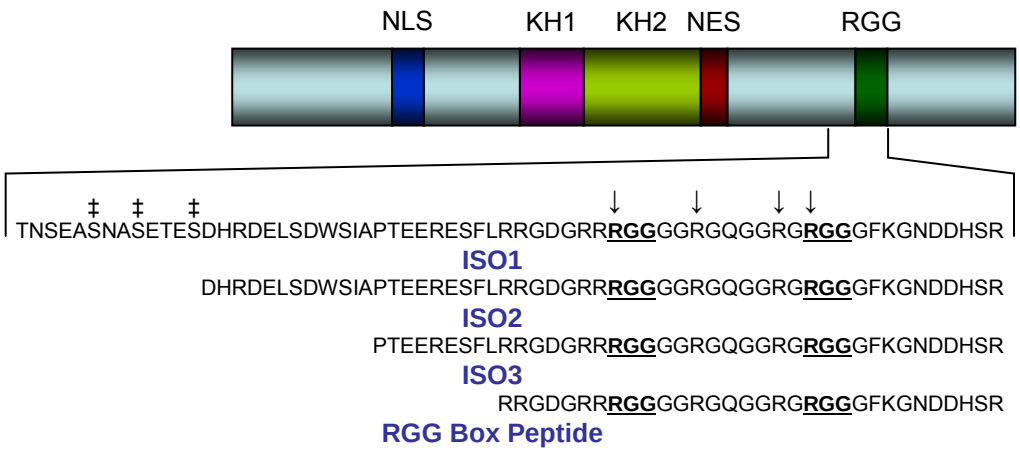

Figure 5. The protein sequence truncation products from the alternative splice acceptor sites at exon 15 of FMR1 mRNA. ISO1 is truncated by 13 residues to form ISO2, truncated another 12 residues to form ISO3. The RGG repeats comprised in the RGG box domain are underlined and bolded. The sites of posttranslational phosphorylation are indicated by double daggers (‡). The region of phosphorylation is lost upon forming ISO2 and ISO3. The sites or posttranslational arginine methylation are indicated by arrows (↓). The sequence of the 32mer synthetic RGG box peptide, and consequently the RGG box domain sequence, is also shown. Adapted from [8, 34, 39].

It has also been shown that FMRP is posttranslationally methylated within its RGG box and that its binding affinity for homoribopolymers (poly(rG), poly (rC), poly (rA), or poly (rU)) changes when the protein is produced in the presence of protein arginine methyltransferases (PRMTs) (Fig 5) [10, 39-41]. The PRMT responsible for methylation is not known, but FMRP is asymmetrically dimethylated indicating that a type I methyltransferase is responsible [40]. It has been proposed that PRMT1 is

responsible for methylating FMRP since this enzyme is responsible for more than 90% of the type I arginine methylation activity in cells, and can methylate peptides containing multiple glycine-arginine-glycine sequences *in vitro* as well as proteins containing multiple glycine-arginine-glycine sequences *in vivo*. It is noteworthy that of the four arginines identified as being asymmetrically dimethylated, two reside on the RGG repeats comprised in the RGG box domain, whereas the other two are the only arginines that reside between these RGG repeats. Moreover, methylation of FMRP reduced its ability to associate with Sc1, a G quadruplex forming synthetic RNA [10]. These results suggest that protein arginine methylation plays an important role in defining the interactions of FMRP with its G quadruplex forming mRNA targets.

1.4 *In vivo* Ribonucleic Acid Targets of the FMRP RGG Box

Several *in vivo* neuronal G quadruplex forming mRNA FMRP targets have been identified, such as the microtubule associated protein 1B (MAP1B) mRNA and semaphorin 3F (S3F) mRNA [4, 6, 17, 31, 42, 43]. In addition, the FMRP mRNA has also been proposed to form a G quadruplex structure which has been shown to be recognized by FMRP [44], leading to the proposal that FMRP could mediate its own translation regulation. However recent evidence shows that FMRP does not regulate its own mRNA translation, but rather its binding to its own mRNA via a G quadruplex structure plays a role in the alternative splicing of this RNA [44]. The MAP1B mRNA, which interacts with FMRP *in vivo*, has been shown to form a G quadruplex structure which is bound by the FMRP RGG box peptide *in vitro* with high affinity and specificity [4, 45-48]. Regulation of MAP1B mRNA translation is of great importance since its

protein product has been shown to be involved in modulating microtubule dynamics, neurite extension and synapse development [4]. S3F mRNA, which has also been shown to interact with FMRP *in vivo*, forms a G quadruplex structure as well, which is bound by the FMRP RGG box peptide *in vitro* with high affinity and specificity [6, 17, 45, 47]. S3F mRNA is an important target of FMRP since the protein it encodes, Sema 3F, plays an important role in brain development by functioning as a chemo-repellant to axon extension, neuronal migration, and the guidance of growth cones [17, 49, 50].

1.5 Model for FMRP Translation Regulator Function

Increasing the ratio of FMRP RGG box peptide to mRNA has been shown by circular dichroism (CD) spectroscopy to result in the unwinding of the RNA G quadruplex structure of both MAP1B mRNA and S3F mRNA [4, 6, 17]. In addition, identical results occurred when using the G quadruplex forming synthetic Sc1 RNA [16]. Though FMRP is mainly found in the cytoplasm, it binds mRNAs in the nucleus and has nucleo-cytoplasmic shuttle activity. In the cytoplasm, FMRP exhibits mRNA chaperone activity, and it is believed to assist in the transport of its mRNAs targets to actively translating ribosomes, leading to its postulated activity as a translational regulator of mRNAs [51-53]. In addition, it has been shown that stimulation of the metabotropic glutamate receptor 5 (mGluR5) on dendritic spines causes a rapid localized increase in translation of FMR1 mRNA, hence an increase in the local concentration of FMRP [38, 54, 55]. The finding that this local protein synthesis was followed by a rapid decrease in FMRP levels back to baseline suggests a dynamic regulation of the FMRP concentration [55]. Based on these findings, Menon et al proposed the following model for FMRP

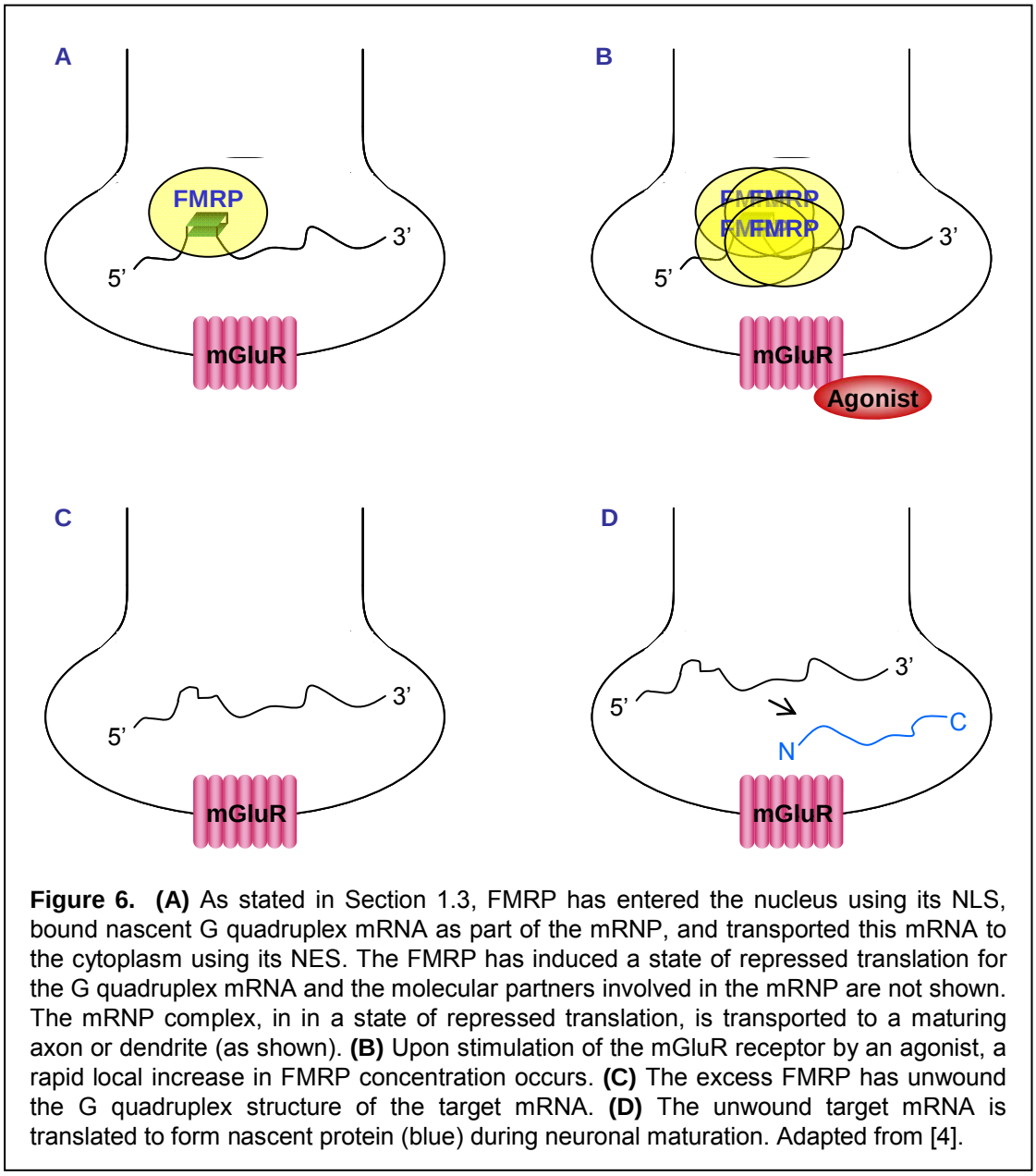

Figure 6. **(A)** As stated in Section 1.3, FMRP has entered the nucleus using its NLS, bound nascent G quadruplex mRNA as part of the mRNP, and transported this mRNA to the cytoplasm using its NES. The FMRP has induced a state of repressed translation for the G quadruplex mRNA and the molecular partners involved in the mRNP are not shown. The mRNP complex, in in a state of repressed translation, is transported to a maturing axon or dendrite (as shown). **(B)** Upon stimulation of the mGluR receptor by an agonist, a rapid local increase in FMRP concentration occurs. **(C)** The excess FMRP has unwound the G quadruplex structure of the target mRNA. **(D)** The unwound target mRNA is translated to form nascent protein (blue) during neuronal maturation. Adapted from [4].

function (Fig 6) [4]: FMRP binds and stabilizes nascent target G quadruplex forming mRNAs in the nucleus and, acting as a translation repressor, transports them in a repressed state to distal sites in the cell. Upon the mGluR5 stimulation by an agonist, there is a rapid increase in the local concentration of FMRP, which creates the high ratio of FMRP to mRNA, and causes the unwinding of the mRNA G quadruplex structure.

Once the G quadruplex structure of the target mRNA is unwound, the ribosome can then proceed with translation.

1.6 Rationale for the Expression of Recombinant FMRP in *Escherichia coli*

Since the discovery of the *FMR1* gene, many studies have attempted to employ recombinant methods to express FMRP. Bacterial, eukaryotic and *in vitro* recombinant expression systems have netted only satisfactory results, with problems involving low levels of FMRP expression and yield, as well as protein precipitation [10, 13, 28, 29, 35, 43, 45, 56-65]. Furthermore, FMRP is known to undergo phosphorylation and arginine methylation, and such posttranslational modifications might occur when using eukaryotic and *in vitro* systems of expression, as the enzymes involved in these pathways are present in such systems [9, 10, 34-41]. However, bacterial cells, such as *Escherichia coli*, do not have the enzymes involved capable of these posttranslational modifications. Therefore, it is of great interest to express recombinant FMRP using bacterial systems because it renders it devoid of phosphorylation and arginine methylation. Producing FMRP devoid of these modifications allows for investigation of the explicit effects of phosphorylation and arginine methylation, individually and simultaneously.

1.7 Specific Aims of the Research

Specific Aim 1: Recombinant Expression in *E. coli*, Purification and Dialysis of Fragile X Mental Retardation Protein Isoforms 1, 2 and 3.

Specific Aim 2: Quantitative Analysis of Binding Activity of Fragile X Mental Retardation Protein Isoforms 1, 2 and 3 to *in vivo* Neuronal Target G quadruplex Forming Messenger Ribonucleic Acid.

Specific Aim 3: Analysis of Translation Regulation Activity of Fragile X Mental Retardation Protein Isoforms 1, 2 and 3 for a Reporter Gene with a G quadruplex Structure in the 5'-Untranslated Region.

1.8 Relevance of the Research

The research performed in this project will increase our understanding of the role played by FMRP in neuronal development and how its absence leads to FXS. We have developed the best protocol to date for the recombinant expression of the three longest FMRP isoforms in *E. coli*, devoid of posttranslational modifications, with subsequent purification, concentration and dialysis conditions. The fact that FMRP produced via our developed method lacks phosphorylation and arginine methylation allows for investigation of the explicit effects of these modifications, both individually and simultaneously, on the various processes that FMRP is involved. We have demonstrated that FMRP ISO1, ISO2 and ISO3 retain biological activity after undergoing the process developed herein. Furthermore, we have shown that as FMRP ISO1 is truncated to form ISO2 and ISO3, due to alternative splicing, the binding affinity becomes tighter for *in vivo* neuronal target G quadruplex mRNA, indicating that neuronal cells utilize alternative splicing as a means to regulate the biological activity of FMRP.

CHAPTER 2: MATERIALS AND METHODS

2.1 Expression of Recombinant FMRP ISO1

The recombinant plasmid pET21a-FMRP, encoding ISO1 fused with a C-terminal 6x histidine affinity tag and an N-terminal T7 affinity tag, was a gift kindly provided by Dr. Bernhard Laggerbauer [60]. The plasmid was transformed into Rosetta 2(DE3) pLysS *E. coli* cells (Novagen), which were cultured at 37 °C, 250 rpm in Luria-Bertani (LB; Fisher Scientific) media containing 200 μg/mL ampicillin (Amp; MP Biomedical) and 15 μg/mL chloramphenicol (Chl; MP Biomedical) and subsequently mixed 1:1 with ultra-pure glycerol and frozen at -80 °C. The concentrations of Amp and Chl were maintained constant throughout cell culturing.

Cells were spread onto an LB + Amp + Chl agar plate using 4-way spread technique and incubated 12 h at 37 °C. Single colonies were picked and cultured (culture 1) in 250 mL LB + Amp + Chl media in a 1 L flask at 37 °C, 250 rpm, 12 h. Eight 2 L flasks (culture 2) were prepared with 500 mL LB + Amp + Chl and 25 mL culture 1 was added to each flask, followed by incubation at 37 °C, 250 rpm until OD_{600} reached 0.8-1.0. The expression of FMRP ISO1 was induced by adding isopropyl β-D-1-thiogalactopyranoside (IPTG) to a final concentration of 1 mM to culture 2 which was then transferred to a separate incubator at 25 °C, 250 rpm for 12 h.

The eight 500 mL culture 2 flasks were equally combined into six 1 L centrifuge flasks and cells were pelleted at 5000 g, 4 °C, 10 min. Pellets were weighed and transferred to individual 50 mL round-bottom polycarbonate centrifuge tubes (Nalgene). A 1:1 mixture of B-PER Bacterial Protein Extraction Reagent (Thermo Scientific) and 2x

lysis buffer (20 mM HEPES, pH 7.5, 600 mM LiCl, 10 mM β-mercaptoethanol, 40 mM imidazole, 10% glycerol) was added at 10 mL buffer/g cells to each pellet, followed by the re-suspension of the pellets by vortexing. Cells were incubated at -20 °C until further purification.

2.2 Purification of Recombinant FMRP ISO1

Resuspended cell pellets were thawed in a 25 °C water bath and then incubated on ice for 30 min to allow lysozyme action encoded by the pLysS cell line. Cells were then sonicated (Branson Sonifier Cell Disruptor 185) three times at a power of 6 for 30 sec with 2 min on ice between bursts. The crude lysate was then centrifuged at 40,000 g, 4 °C, 30 min. A 10 cm x 1.5 cm diameter column was loaded with 10 mL Ni-NTA Superflow resin slurry (Qiagen) at 4 °C and equilibrated with 5 column volumes of equilibration buffer 1 (10 mM HEPES, pH 8.0, 300 mM LiCl, 5 mM β-mercaptoethanol, 5% glycerol, 20 mM imidazole) at 2 mL/min using the BioRad BioLogic LP system. The entire clarified crude supernatant was loaded onto the column at a flow rate of 0.5 mL/min, followed by washes performed at a rate of 2 mL/min: 5 column volumes of equilibration buffer 1, 10 column volumes of equilibration buffer 2 (same components as equilibration buffer 1 except at pH 7.0), and 10 column volumes of wash buffer 1 (10 mM HEPES, pH 7.5, 300 mM LiCl, 5 mM β-mercaptoethanol, 5% glycerol, 100 mM imidazole). An additional wash step was performed, at a flow rate of 1 mL/min with wash buffer 2 (10 mM HEPES, pH 7.5, 300 mM LiCl, 5 mM β-mercaptoethanol, 5% glycerol, 250 mM imidazole). Pure FMRP ISO1 was eluted at a flow rate of 1 mL/min with elution buffer (10 mM HEPES, pH 7.5, 300 mM LiCl, 5 mM β-mercaptoethanol,

5% glycerol, 500 mM imidazole), collecting 15 3 mL fractions. Immediately after elution, ethylenediaminetetraacetic acid (EDTA) was added to each collected fraction to a final concentration of 1 mM and the fractions were stored at 4 °C until dialysis. Fractions from the elution were analyzed via 10% tris-glycine sodium dodecyl sulfate-polyacrylamide gel electrophoresis (SDS-PAGE) and visualized by Coomassie blue stain to assure purity (Fig 7).

2.3 Concentration of Recombinant FMRP ISO1

The concentration protocol was adapted from [66]. A sterile 50 mL beaker was pre-chilled on ice and elution fractions 5-8, containing the highest concentration of FMRP ISO1, were pooled therein. Dialysis tubing of 3500 MWCO, 29.3 mm diameter (Fisher Scientific) was washed in sterile dH_2O and filled with polyethylene glycol 20,000 (J.T. Baker) such that the polyethylene glycol consumed approximately 30% of the available inner volume to allow for expansion. The filled tubing was immersed completely into the beaker containing FMRP ISO1. After pooling FMRP ISO1, the volume for concentrating was 12 mL and the protein was concentrated to a final volume of approximately 3 mL.

2.4 Dialysis of Recombinant FMRP ISO1

For the purpose of the mRNA binding experiments that were monitored by fluorescence spectroscopy, FMRP ISO1 had to be devoid of imidazole. All dialysis buffers were prepared two days in advance of use, without adjusting the pH, and allowed to equilibrate overnight at 4 °C. The pH adjustments occurred one day prior to use and

allowed to finish equilibration over night at 4 °C. Dialysis tubing of 10,000 MWCO, 7.5 mm diameter (Spectra/Por) was washed with sterile dH_2O and the concentrated FMRP ISO1 was added. All dialysis buffers were, volume-wise, approximately 667:1 to FMRP ISO1 and incubations in the respective dialysis buffer occurred for 12 h at 4 °C. Each dialysis buffer (2L) contained 10 mM HEPES, pH 7.5, 300 mM LiCl, 5 mM β-mercaptoethanol, 5% glycerol, 1 mM EDTA and variable imidazole concentrations, as follows: the first dialysis buffer contained 200 mM imidazole, the second contained 100 mM imidazole, the third contained 50 mM imidazole and the fourth contained no imidazole. After dialysis, the concentration of FMRP ISO1 was determined to be 50 μM by absorbance at 280 nm using an extinction coefficient of 46370 M^{-1} cm^{-1} adapted from [67, 68]. The purity and retention of the protein were analyzed by 10% tris-glycine SDS-PAGE and visualized by Coomassie blue stain (Fig 8).

2.5 Mass Spectrometry Analysis of FMRP ISO1

The identity of FMRP ISO1 was confirmed using peptide mass fingerprinting (Genomics and Proteomics Core Laboratories, University of Pittsburgh) (Table 1). FMRP ISO1 from a 10% SDS-PAGE gel was excised and trypsin digested followed by analysis via matrix-assisted laser desorption/ionization-time of flight-mass spectrometry (MALDI-TOF-MS). The five MALDI-TOF-MS characterized amino acid sequences matched that found in FMRP ISO1.

2.6 Production of the pET-21a Plasmid Encoding ISO2 and ISO3

The pET-21a-FMRP plasmid, encoding ISO1 fused with a C-terminal 6x histidine affinity tag and an N-terminal T7 affinity tag, was a gift provided by Dr. Bernhard Laggerbauer [60]. The truncations of *FMR1* cloned into pET-21a, which encodes ISO1, to form the genes to express ISO2 and ISO3 were performed by GenScript and confirmed by DNA sequencing. The affinity tags remained intact after the gene truncations. The plasmids containing the genes encoding ISO2 and ISO3 were also restriction digested with XhoI to confirm the changes in size corresponding to the truncations and analyzed by 1% agarose gel electrophoresis and visualized by ethidium bromide stain (Fig 9).

2.7 Expression, Purification, and Dialysis of Recombinant FMRP ISO2 and ISO3

The pET-21a plasmids encoding ISO2 and ISO3 were transformed into Rosetta2 (DE3) pLysS *E. coli* cells. The protocol developed for the expression, purification, concentration and dialysis of FMRP ISO1 was applied to ISO2 and ISO3. After dialysis, the concentration of FMRP ISO2 and ISO3 were determined to be similar to that of ISO1 by absorbance at 280 nm using extinction coefficients of 46370 M^{-1} cm^{-1} and 40680 M^{-1} cm^{-1}, respectively, adapted from [67, 68]. Successful production of pure, dialyzed FMRP ISO2 and ISO3 was confirmed by 10% tris-glycine SDS-PAGE analysis and visualized by Coomassie blue stain (Fig 10).

2.8 Analysis of FMRP ISO1, ISO2 and ISO3 Binding Activity to G quadruplex Forming mRNA

In order to ensure that FMRP ISO1 maintained mRNA binding activity after the aforementioned processes, we performed a fluorescence RNA binding assay according to [6, 17]. Briefly, the G quadruplex forming semaphorin 3F mRNA (S3F-sh) fragment was labeled by the highly fluorescent purine analog 2-aminopurine (2-AP) at position 8, producing S3F-sh_8AP (Dharmacon, Inc) (Figs 11, 12) [17]. The replacement of adenine with 2-aminopurine has been shown to not disrupt G quadruplex formation and binding interactions of various mRNAs with the RGG box peptide [4, 6, 17]. The fluorescence spectroscopy experiments were performed on a J.Y. Horiba Fluoromax-3 equipped with a variable temperature control in the sample chamber and a 3 mm path-length quartz cuvette (Starna Cells) in a 150 μL final volume. The excitation wavelength was set at 310 nm and the emission spectrum was recorded in the range of 330-450 nm with a bandpass of 5 mm for both the excitation and emission monochromators.

The binding was measured by titrating either FMRP ISO1, ISO2 or ISO3 into a fixed concentration of 150 nM S3F-sh_8AP mRNA (in 10 mM cacodylic acid, pH 6.5, 150 mM KCl) at 25 °C. The samples were incubated for 10 min after each addition of each increment of the respective FMRP isoform. The binding dissociation constant, K_d, was determined by plotting the normalized S3F-sh_8AP mRNA steady state fluorescence intensity at 371 nm as a function of the respective FMRP isoform concentration and fitting the resultant binding curves to the equation [17]:

$$F = 1 + \left(\frac{I_B}{I_F} - 1 \right) \bullet \frac{\left(K_d + [P]_t + [RNA]_t \right) - \sqrt{\left(K_d + [P]_t + [RNA]_t \right)^2 - 4 \bullet [P]_t \bullet [RNA]_t}}{2 \bullet [RNA]_t} \quad (1)$$

where I_B and I_F are the steady state fluorescence intensity of the bound and free S3F-sh_8AP mRNA, $[RNA]_t$ is the total concentration of S3F-sh_8AP mRNA, and $[P]_t$ is the total respective FMRP isoform concentration. The best-fit curve and subsequent K_d and R^2 values for the respective FMRP isoform binding S3F-sh_8AP mRNA were generated using Origin 7.0 (Fig 13). The experiments were repeated in triplicate and bovine serum albumin (BSA) was also similarly titrated as a negative control (Fig 13A).

2.9 Secondary Structure Predictions of FMRP ISO1, ISO2 and ISO3

The amino acid sequence of each FMRP isoform was input for secondary structure prediction using Porter, nnPredict, Jnet, and ProteinPredict computational servers (Fig 14) [69-73].

2.10 Production of the Luciferase Reporter Gene Assay Plasmid Construct

The luciferase assay reporter construct was designed based on [26]. The following DNA sequence was cloned into the multiple cloning site of the pUC18 plasmid by GenScript: minimal T7 RNA polymerase promoter (25 bases), followed downstream by the DNA sequence encoding the microtubule associated protein 1B (MAP1B) mRNA 5'-UTR mRNA sequence shown to form the G quadruplex structure (34 bases), followed downstream by a portion of the luciferase 5'-UTR that immediately precedes the luciferase gene (*luc*) start codon (18 bases), and then *luc* (Fig 15). The distance between the end of the T7 promoter and the *luc* start codon was required to be less than 100 bases in order to ensure expression of luciferase. In addition, an EcoRI restriction digest site was incorporated immediately following the stop codon of *luc* to allow linearization of

the plasmid prior to *in vitro* transcription. The pRM10 plasmid encodes mRNA with the MAP1B mRNA G quadruplex sequence in its 5'-UTR, while pRM11 encodes a mutated MAP1B mRNA G quadruplex sequence incapable of forming the G quadruplex structure (Fig 15). The pRM12 plasmid does not contain any portion of the MAP1B sequence (Fig 15).

2.11 Purification and EcoRI Digest of the pRM10, prM11 and pRM12 Plasmids

The pRM10, pRM11 and pRM12 plasmids were transformed into and cultured using BL21 Gold *E. coli* cells for the replication of the plasmids. The cells were cultured at 37 °C, 250 rpm in LB + 200 μg/mL Amp and then mixed 1:1 with ultra-pure glycerol and frozen at -80 °C. Cell were spread onto an LB + Amp agar plate using 4-way spread technique and incubated 12 h at 37 °C. Single colonies were picked and cultured in 250 mL LB + Amp media in a sterile 1 L Erlenmeyer flask at 37 °C, 250 rpm, 12 h. The respective pRM plasmid was purified using the E.Z.N.A. Endo-Free Plasmid Maxi Kit (Omega Bio-Tek). The manufacturer's Spin Protocol was employed, and the respective plasmid was eluted using 2.25 mL of Endo-Free Elution Buffer and analyzed for purity by 1% agarose gel electrophoresis and visualized by ethidium bromide stain (Fig 16). The typical yield was 150 μg/mL and purified plasmids were stored at -20 °C.

The respective purified plasmid DNA was thawed on ice during preparation for the EcoRI restriction enzyme digest. The restriction digest mixture was prepared in a 500 μL Eppendorf tube and contained 42 μL of ~150 μg/mL respective pRM plasmid, 5 μL 10x EcoRI NEBuffer (New England Biolabs), and 3 μL EcoRI restriction enzyme solution (New England Biolabs). The restriction digest mixture was incubated at 37 °C,

3.5 h using the MJ Mini Personal Thermocycler (Bio-Rad) and successful restriction digest was analyzed by 1% agarose gel electrophoresis and visualized by ethidium bromide stain (Fig 16).

2.12 Ethanol Precipitation Purification of the EcoRI Digested pRM plasmids

The reaction digest mixture was transferred to a 1.5 mL Eppendorf tube. The respective digested pRM plasmid was purified by ethanol precipitation by adding $1/20^{th}$ volume of 0.5 M EDTA, $1/10^{th}$ volume 3 M sodium acetate, and then 2 volume of ice-cold absolute ethanol. After addition of ethanol, the mixture was incubated at -20 °C for 30 min then centrifuged at 13,000 g for 15 min to pellet the respective digested plasmid. The supernatant was decanted, and the pellet was centrifuged at 13,000 g for 1 min. The remaining liquid was removed by a fine-tipped pipette set at a 10 µL volume. The respective digested pRM plasmid was resuspended in TE buffer (10 mM Tris, pH 8.0, 1 mM EDTA) to a final concentration of 1 µg/mL (typically requiring ~150 uL TE) and analyzed by 1% agarose gel electrophoresis for successful purification and visualized by ethidium bromide stain (Fig 16).

2.13 *In vitro* Transcription of the pRM Plasmids and Purification of the Resultant pRM mRNA Transcripts

The *in vitro* transcription of the respective restriction digested ethanol precipitated pRM plasmid was performed according to the manufacturer protocol using the mMessage mMachine T7 Kit (Ambion). The *in vitro* transcription reaction mixture was assembled according to the manufacturer instructions, except 1 µg of respective restriction digested

ethanol precipitated pRM plasmid template was used and the incubation occurred for 2.5 h at 37 °C. Following *in vitro* synthesis of the respective pRM transcript, TURBO DNase was added to the reaction mixture and the reaction was incubated for 25 min at 37 °C. The respective pRM mRNA was purified by ethanol precipitation as described in section 2.12 of the Materials and Methods, and the respective mRNA precipitated pellet was resuspended in 50 μL TE buffer and KCl was added to 10 mM from a 4 M stock. The effectiveness of the *in vitro* transcription reaction and mRNA purification were assessed by 1% agarose gel electrophoresis and visualized by ethidium bromide stain (Fig 16).

2.14 *In vitro* Translation of the Respective pRM mRNA Transcripts

The *in vitro* translation of the respective purified pRM transcript was performed according to the manufacturer's protocol using the Rabbit Reticulocyte Lysate System (Promega). The protocol calls for an annealing step for the mRNA at 60 °C prior to *in vitro* translation to unfold any potential mRNA secondary structures. Hence, before their addition to the translation reaction, the pRM plasmids were incubated in the presence of 10 mM KCl for 3 min to allow the folding of the mRNA into the G quadruplex structure upon cooling. The amino acid mixture minus leucine, the amino acid mixture minus methionine, and the RNasin ribonuclease inhibitor were added according to the manufacturer's protocol (Promega), and nuclease-free water was added to adjust the final volume to 50 μL. An aliquot containing the respective mRNA was added to a corresponding aliquot of FMRP ISO1 such that the ratios of FMRP:pRM mRNA were 2:1, 1:1 and 0:1 and incubated at 25 °C for 20 min. The various respective FMRP

isoform titration aliquots were diluted as needed in such a way that the volume of every aliquot was identical to avoid the effects of dilution on luminescence emission. The entire FMRP ISO1-pRM mRNA mixture was added to the *in vitro* translation reaction mixture. Identical aliquots of the RRL were added to each reaction, followed by incubation at 30 °C for 1.5 h.

The luminescence emission intensity was measured at 560 nm using a Veritas Microplate Luminometer (Turner Biosystems). The 4.5 μL room-temperature aliquots of the respective RRL *in vitro* translation reactions were added to an opaque 96-well plate, and the auto-injections system of the instrument delivered 90 μL of room temperature luciferase assay reagent (Promega) to each well. The *in vitro* translated luciferase in the RRL was incubated with the luciferase assay reagent for 10 sec prior to analysis of luminescence emission intensity. The luminescence emission intensity was normalized relative to that from the positive control pRM12 construct.

CHAPTER 3: RESULTS AND DISCUSSION – RECOMBINANT EXPRESSION IN *E. COLI*, PURIFICATION AND DIALYSIS OF FMRP ISOFORMS 1, 2 AND 3

3.1 Expression and Purification of Recombinant FMRP ISO1

Since the discovery of the FMR1 gene, the recombinant expression of FMRP in *E. coli* has been continuously pursued, however the results of these efforts have been less than satisfactory. Those who have attempted recombinant expression in *E. coli* have experienced problems involving low levels of FMRP expression and yield as well as protein precipitation [10, 28, 29, 45, 57, 59-63, 74]. In trying to circumvent these problems, other studies have employed eukaryotic cell lines and *in vitro* transcription and translation systems, but they also had limited success [13, 35, 43, 56-59, 61-64, 74]. Furthermore, FMRP is known to undergo phosphorylation and arginine methylation, and such posttranslational modifications are likely concomitant when using eukaryotic and *in vitro* systems of expression, as the enzymes involved in these modification pathways are present in such systems [9, 10, 34-41]. Thus, to elucidate the explicit effects of these posttranslational modifications on FMRP activity, both individually and simultaneously, the expression of FMRP in the prokaryotic *E. coli* is vital.

Initially we attempted the FMRP ISO1 expression using the BL21 Gold (DE3) *E. coli* cell line; however these experiments were not successful due to the low expression of the protein. One cause for this poor FMRP ISO1 expression could have been codon bias. The expression of FMRP ISO1 was then carried out using the Rosetta2 (DE3) pLysS *E. coli* cell line. There exists seven transfer RNAs (tRNAs) that are not normally expressed in *E. coli*, hence those seven codons are not recognized during translation. The Rosetta2

(DE3) pLysS cell line contains the pRARE2 plasmid, encoding those seven tRNAs. Analysis of the *FMR1* sequence revealed that codon bias would have to be overcome. This was of particular concern since of the seven compensated tRNAs, three correspond to arginine codons and one corresponds to glycine and the RNA binding domain of interest in the studies, the RGG box domain, is rich in arginine and glycine (Fig 2B). Moreover, the three arginine codons appear a combined total of 35 times and the glycine codon appears 25 times. In addition to compensating for codon bias, the utilization of the pLysS cell line allows the cells to endogenously express lysozyme, eliminating the need to add exogenous lysozyme and reducing the time necessary for the protein purification procedure. Based on the tendency for FMRP to precipitate, the endogenous lysozyme also enables a gentler lysis of the cells during the purification.

The transformed cells were grown at 37 °C until OD_{600} was 0.8-1.0 and following induction with IPTG, the cultures were grown for an additional 12 h at 25 °C. Following cell harvesting and lysis, Ni^{2+} affinity chromatography was employed for the purification process. Initially, the eluted fractions contained other protein impurities, which we attempted to remove using additional steps, such as, but not limited to, gel filtration chromatography, NH_4SO_4 precipitation, or different Ni^{2+} affinity resin, however these resulted in either protein loss or minimal increase in purity. By varying the buffer components, imidazole concentration and pH during the optimization of the lysis and wash steps of the Ni^{2+} affinity chromatography, pure FMRP ISO1 was successfully produced using only the Ni-NTA resin column (Fig 7). Utilizing single-column affinity chromatography reduces the necessary amount of time for purification, allowing analyses of FMRP sooner, and decreases the quantity of steps that could be required, all of which

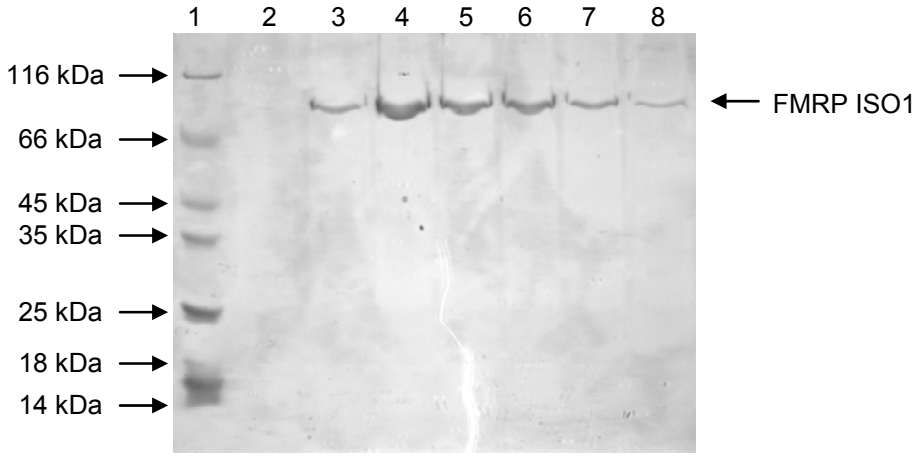

Figure 7. 10% tris-glycine SDS-PAGE analysis of FMRP ISO1 purity after the Ni-NTA affinity chromatography developed herein. FMRP ISO1 is not expressed strongly enough in the presence of IPTG to be visibly distinguished from other protein bands in the cleared crude supernatant hence that sample is not shown. Lane 1: EZ-Run protein marker (Fisher Scientific). Lanes 2-8: eluted pure FMRP ISO1 fractions 4-10, respectively. Visualized by Coomassie blue stain.

reduce the chance of protein precipitation. Furthermore, these studies revealed that the long term storage of FMRP ISO1 is optimal at 4 °C in the presence of the elution buffer containing 500 mM imidazole, 5% glycerol, and 1 mM EDTA. Glycerol has been shown to stabilize proteins, and is routinely in many situations, such as protein refolding or crystallization [75]. Although not well understood, it has been proposed that glycerol induces protein compaction, reduces protein flexibility, stabilizes partially unfolded intermediates, and affects both native and non-native protein aggregation. In addition, it was shown that imidazole exhibits chaperone-like activity by enhancing green fluorescent protein refolding and by suppressing heat-induced green fluorescent protein aggregation [76]. It was proposed that imidazole binds to and blocks the exposure of nonnative solvent-exposed hydrophobic surfaces of protein folding intermediates, possibly by

imidazole binding solvent-exposed aromatic amino acid residues through stacking interactions.

3.2 Mass Spectrometry Confirmation of FMRP ISO1 Expression

Upon obtaining pure FMRP ISO1, MALDI-TOF-MS analysis was one of the two methods used to confirm successful FMRP ISO1 expression and purification. Pure FMRP ISO1 from a 10% SDS-PAGE gel was excised, trypsin digested and MALDI-TOF-MS analyzed at the Genomics and Proteomics Core Laboratories at the University of Pittsburgh. The five peptide fragments detected were identical to FMRP based on matches within the Xcalibur mass spectrometry database (Table 1). The five fragments detected are characteristic of several FMRP isoforms, hence based on these results combined with the DNA sequencing of the pET21a-FMRP plasmid and the correct molecular weight of expressed FMRP ISO1 was successfully expressed.

Table 1. Results from the MALDI-TOF-MS sequence analysis of trypsin digested FMRP ISO1

Peptide Sequence	Observed Mass	Expected Mass	Δ Mass	Protein Identified
(K)LIQEIVDK(S)	958.13403	958.1400	-0.00597	FMRP
(K)NVPQEEEIM*PPNSLPSNNSR(V)	2269.43498	2269.4425	-0.00752	FMRP
(R)VLVASSVVAGESQKPELK(A)	1842.12671	1842.1375	-0.01079	FMRP
(R)EDLM*GLAIGTHGANIQQAR(K)	2012.23703	2012.2433	-0.00627	FMRP
(K)AWQGM*VPFVFVGTK(D)	1583.87812	1583.8837	-0.00558	FMRP

* indicates oxidized methionine

3.3 Concentration and Dialysis of Recombinant FMRP ISO1

The dialysis tubing concentration method was adapted for the concentration of FMRP ISO1 [66]. This method drastically reduced the FMRP ISO1 precipitation and loss due to membrane adsorption found when attempting other concentration methods, such as lyophilization, NH_4SO_4 precipitation, and centrifugal concentration filter devices with regenerated cellulose or polyethersulfone membranes. In addition, the optimization of the process revealed that concentration of ISO1 in the presence of hydrogen bonding-capable agents, such as glycerol and imidazole, inhibited precipitation [75, 76]. Based on this, FMRP ISO1 was concentrated while in the elution buffer containing 500 mM imidazole and 1 mM EDTA.

As previously stated, the presence of hydrogen bonding-capable agents, such as imidazole and EDTA, reduced FMRP ISO1 precipitation. The concentration of imidazole to this point is 500 mM, too high to accurately represent *in vivo* conditions, yet the presence of imidazole reduces FMRP ISO1 loss. Additionally, the presence of imidazole is not compatible with the fluorescence spectroscopy mRNA binding assay because imidazole absorbs at 280 nm and the excitation of the 2-AP label occurs at 310 nm. Hence, the dialysis conditions herein were developed for the gradual removal of imidazole which resulted in minimal loss through precipitation. Initially, the concentrated FMRP ISO1 is in elution buffer containing 500 mM imidazole, 5% glycerol and 1 mM EDTA. Every dialysis step was performed at 4 °C for 12 h with 2 L of buffer that contained 10 mM HEPES, pH 7.5, 300 mM LiCl, 5 mM β-mercaptoethanol, 5% glycerol, 1 mM EDTA and varying concentrations of imidazole. The approximate 3 mL concentrated FMRP ISO1, in elution buffer with 500 mM imidazole and 1 mM EDTA,

was transferred to a dialysis buffer containing 200 mM imidazole, followed by 100 mM imidazole, then 50 mM imidazole and zero imidazole. Following concentration and imidazole removal, analysis by SDS-PAGE shows that FMRP ISO1 remains pure and free of proteolytic degradation (Fig 8). After purification and dialysis, the concentration of FMRP ISO1 was typically 50 μM in a volume of approximately 3 mL.

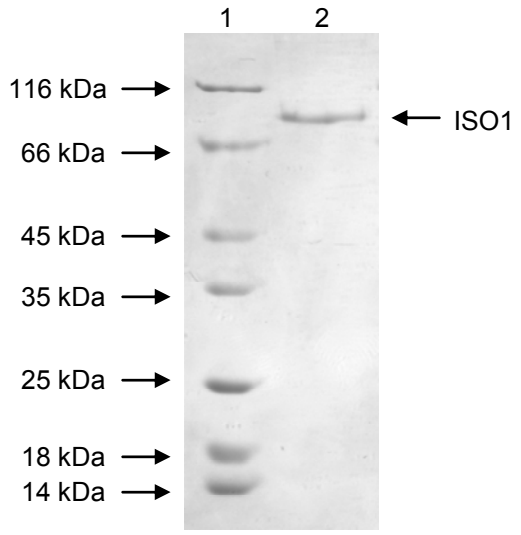

Figure 8. 10% tris-glycine analysis of FMRP ISO1 after the purification, concentration and dialysis processes and ready for binding analysis with G quadruplex mRNAs. Lane 1: EZ-Run protein marker. Lane 2: dialyzed FMRP ISO1. Visualized by Coomassie blue stain.

3.4 Recombinant Expression and Purification of FMRP ISO2 and ISO3

The naturally occurring splice acceptor sites at exon 15 result in the three longest FMRP isoforms, with ISO1 being truncated by 13 residues to form ISO2, and truncated an additional 12 residues to form ISO3 (Fig 5) [27-30]. The plasmids encoding for FMRP ISO2 and ISO3 were prepared by GenScript, starting from the plasmid encoding for FMRP ISO1. The successful deletion of the sequences of *FMR1* to yield FMRP ISO2

and ISO3 was confirmed by XhoI restriction enzyme digest and 1% agarose gel electrophoresis (Fig 9). The two XhoI cut sites appear on each side of the region encoding the RGG box and the *FMR1* truncation sites, resulting in a relatively small fragment by which the small quantity of bases deleted (39 total for ISO2 and 75 total for ISO3) whose elimination could be detected on an agarose gel. The genetic deletions were also verified by sequencing the coding region of the respective plasmids.

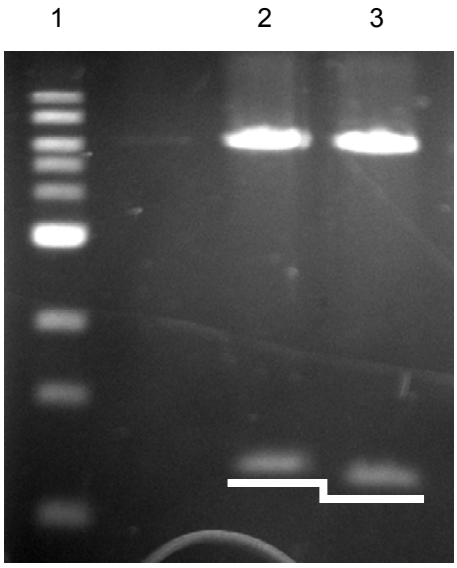

Figure 9. 1% agarose gel electrophoresis of XhoI digested pET-21a plasmids containing the genes encoding FMRP ISO2 and ISO3. Lane 1: DNA marker. Lane 2: ISO2 encoding plasmid. Lane 3: ISO3 encoding plasmid. The size difference resulting from gene truncation is reflected in the migration distance and enhanced by the white underline. Visualized by ethidium bromide.

The truncations of FMRP ISO1 of 12 and 25 residues to form ISO2 and ISO3, respectively, did not alter the properties of the protein such that the protocol developed for the production of ISO1 could not be applied to ISO2 and ISO3. Hence, pure FMRP

ISO2 and ISO3 were expressed and dialyzed by following the protocol described above for the recombinant expression and purification of FMRP ISO1 (Fig 10).

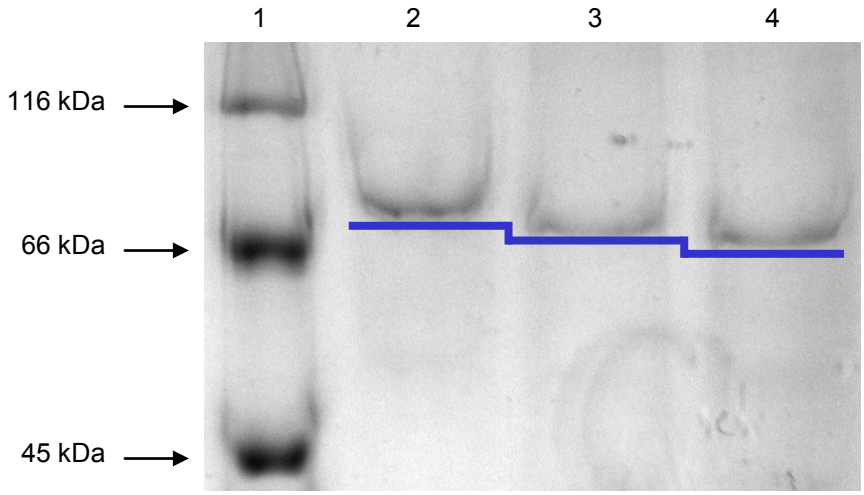

Figure 10. 10% SDS-PAGE analysis of the truncation to FMRP ISO1 to form ISO2 and ISO3. Analysis occurred post-dialysis. Lane 1: EZ-Run protein marker. Lanes 2-4: FMRP ISO1, ISO2 and ISO3, respectively. The size differences resulting from FMRP truncations are reflected in the migration distance and enhanced by the blue underline. Visualized by Coomassie blue stain.

CHAPTER 4: RESULTS AND DISCUSSION – QUANTITATIVE ANALYSIS OF BINDING ACTIVITY OF FMRP ISOFORMS 1, 2 AND 3 TO *IN VIVO* NEURONAL TARGET G QUADRUPLEX FORMING MRNA

4.1 FMRP ISO1, ISO2 and ISO3 Binding Activity to G quadruplex Forming mRNA

To confirm that the recombinant FMRP ISO1 retained activity throughout the developed protocol herein for binding G quadruplex forming mRNA, its ability to bind G quadruplex mRNA was evaluated using fluorescence spectroscopy [4, 6, 16, 17, 45].

Depending on the particular RNA sequence, the formation of the G quadruplex structure requires K^+ ions in different concentrations. Based on the variability of the required K^+ concentration, the binding assay buffer must have K^+ concentration flexibility; hence the FMRP isoforms must be in a buffer devoid of K^+. Moreover, the G quadruplex can form in the presence of Na^+ ions but this is thermodynamically less stable relative to when K^+ is present [18]. Thus, Li^+ was employed throughout the purification and dialysis processes in place of the routinely used K^+ and Na^+ buffer counterions.

The mRNA we employed (S3F-sh_8AP) in the respective FMRP fluorescence spectroscopy binding assay was derived from the semaphorin 3F mRNA, which encodes for the Sema 3F protein (Fig 11) [17]. The Sema 3F protein is expressed in cerebellar granule cells and plays an important role in brain development by functioning as a chemo repellant to axon extension, neuronal migration and growth cone guidance [49, 50]. Previous studies have shown that the S3F mRNA is an *in vivo* neuronal binding target of FMRP and that, *in vitro*, S3F-sh_8AP mRNA folds into a G quadruplex structure which

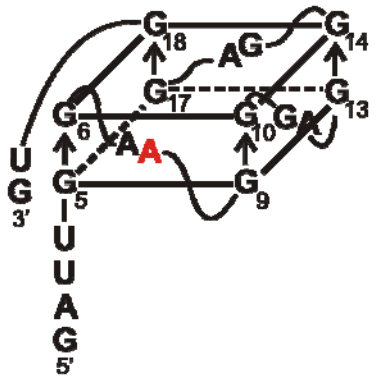

5'-GAUUGGAAGGGAGGGAGGUG-3'

Figure 11. Left figure shows the proposed G quadruplex structure of S3F-sh_8AP mRNA with the location of the 2-aminopurine fluorescent label in red [17]. Right figure shows the sequence of S3F-sh_8AP mRNA with the 2-aminopurine fluorescent label in red and the guanine bases involved in G quadruplex formation underlined. The adenine analog 2-aminopurine was substituted for a naturally occurring adenine in the sequence.

is bound with high affinity and specificity by a synthetic FMRP RGG box peptide (Fig 5) [6, 17, 45, 77]. S3F-sh_8AP mRNA was labeled at position 8 by the highly fluorescent adenine analog 2-AP (Fig 12). This adenine analog was substituted for a naturally occurring adenine in the S3F mRNA, and 2-AP has been shown to be non-perturbing to both the folding of the G quadruplex mRNA structure and binding by the synthetic RGG box peptide [4, 6, 17]. The fluorescence emission of 2-AP is sensitive to changes in its local microenvironment (Fig 12), such as stacking on other bases and protein binding [78]. Increasing amounts of a respective FMRP isoform were titrated against a fixed concentration of the labeled mRNA (150 nM), monitoring the steady-state fluorescence changes of the 2-AP reporter at 371 nm (Fig 13). By fitting the respective resultant binding curves with Equation 1 (Materials and Methods) using Origin software, the binding dissociation constants (K_d) for the respective FMRP isoform were determined (Fig 13) (Table 2). These dissociation constants are in the nM range, being comparable, but not identical, to the value previously reported for the binding of the synthetic FMRP

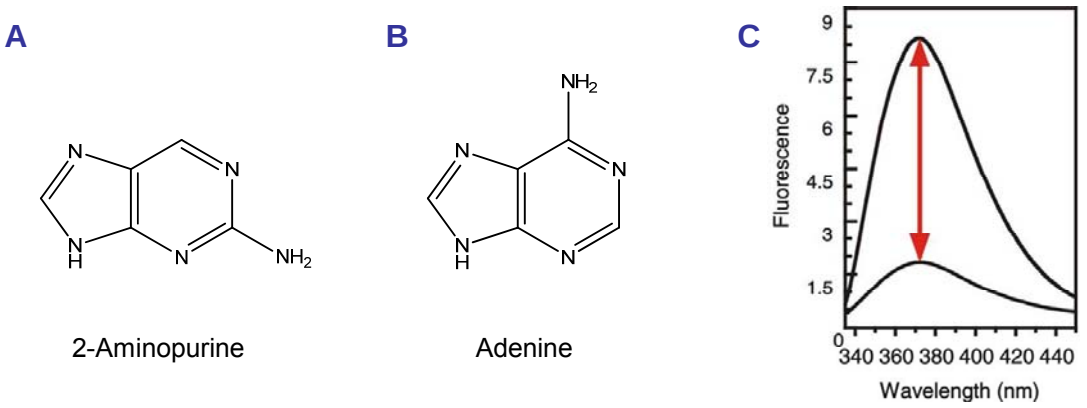

Figure 12. (A) Molecular structure of the adenine analog fluorescent label 2-aminopurine. **(B)** Molecular structure of adenine. **(C)** Changes in the 2-aminopurine fluorescence emission intensity from changes in its local microenvironment.

RGG box peptide to this mRNA (Fig 5) (Table 2) [17]. Additionally, the K_d values of FMRP ISO1, ISO2 and ISO3 for the G quadruplex forming S3F-sh_8AP mRNA are also in the same range with the K_d of the synthetic FMRP RGG box peptide for the G quadruplex forming MAP1B_19AP mRNA, at 20.1 ± 6.4 nM [4]. As a negative binding control, BSA was titrated into S3F-sh_8AP mRNA resulting in a minimal change (less than 10%) of the steady-state fluorescence of the 2-AP reporter (Fig 12A).

Table 2. Results of the fluorescence binding assays of various FMRP isoforms to G quadruplex forming S3F-sh_8AP mRNA

FMRP Isoform	K_d (nM)	R^2
ISO1	104 ± 11	0.995
ISO2	46 ± 4	0.996
ISO3	25 ± 3	0.991
RGG box peptide	1.0 ± 0.4	-

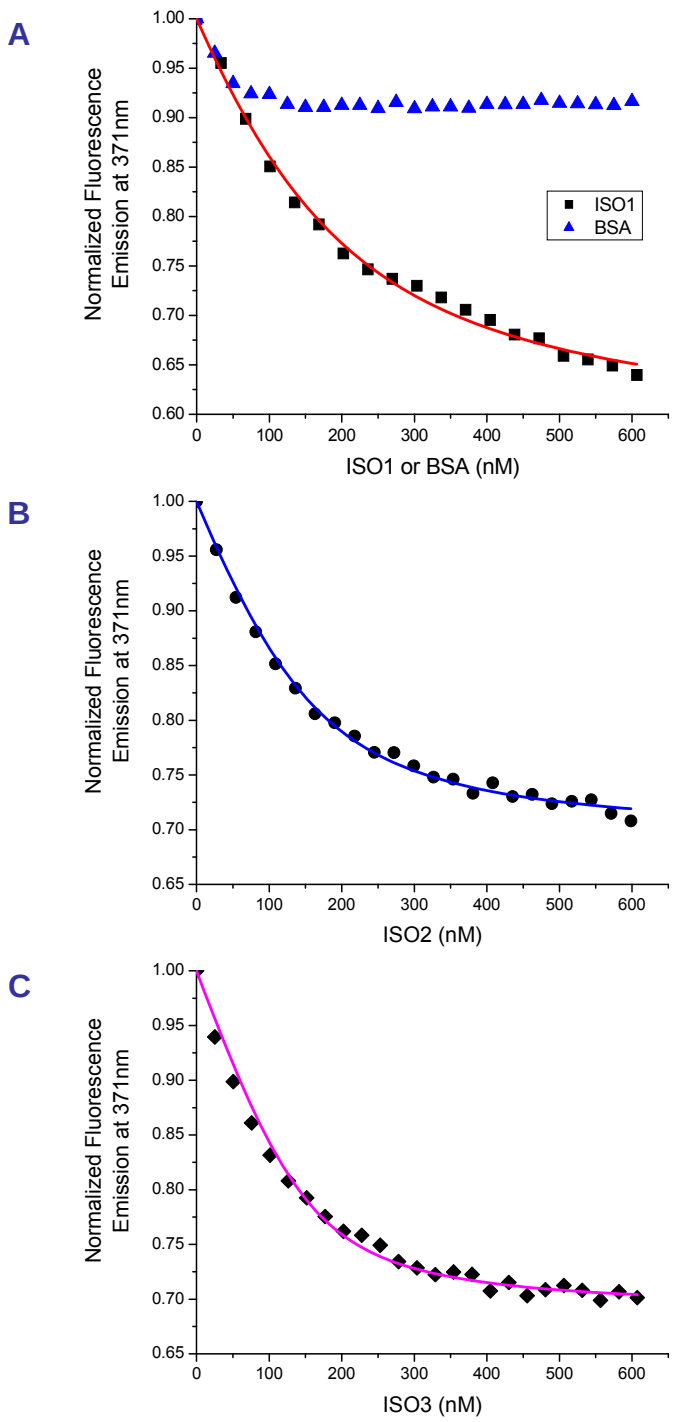

Figure 13. (A) (■) Best-fit curve from the steady-state fluorescence spectroscopy emission of S3F-sh_8AP mRNA at 371 nm as ISO1 is titrated and binding. The result was a K_d of 104.1 ± 10.9 nM and R^2 value of 0.995. (▲) The negative binding control from the steady-state fluorescence spectroscopy emission of S3F-sh_8AP mRNA at 371 nm as BSA is titrated. **(B)** Best-fit curve of S3F-sh_8AP mRNA at 371 nm as ISO2 is titrated and binding. The result was a K_d of 45.7 ± 4.1 nM and R^2 value of 0.996. **(C)** Best-fit curve of S3F-sh_8AP mRNA at 371 nm as ISO3 is titrated and binding. The result was a K_d of 24.7 ± 3.3 nM and R^2 value of 0.991.

4.2 Analysis of the Effects of FMRP Truncations via Alternative Splicing on the Binding Activity to G quadruplex Forming mRNA

Efforts have not yet yielded a structure for any FMRP isoform; additionally, there are no known structures for any RGG box domain-containing protein. Moreover, the RGG box domain and surrounding region are thought to be unstructured, and it is thought that the RGG box becomes structured during the binding event with the G quadruplex mRNA [47]. The three longest FMRP isoforms studied here are products of the three alternative splice acceptor sites at exon 15, and these alternative splice products are the result of truncations that occur in close proximity to the RGG box domain (Fig 5) [27-30]. Our fluorescence spectroscopy binding experiments indicate that as FMRP ISO1 is truncated by 13 residues to form ISO2, and then another 12 residues to form ISO3, the binding affinity of the FMRP RGG box domain for G quadruplex mRNA increases (Table 2).

In effort to elucidate the rationale for the righter K_d as FMRP truncation occur, we performed secondary structure predictions for FMRP ISO1, ISO2 and ISO3 (Fig 14) [69-73]. Of the four secondary structure predictions utilized, at least two had to agree in order to be considered valid for these studies, according to the predictions from the Porter, nnPredict, Jnet, and ProteinPredict computational servers (Fig 14) [69-73] According to the predictions, the RGG box domain and surrounding region are

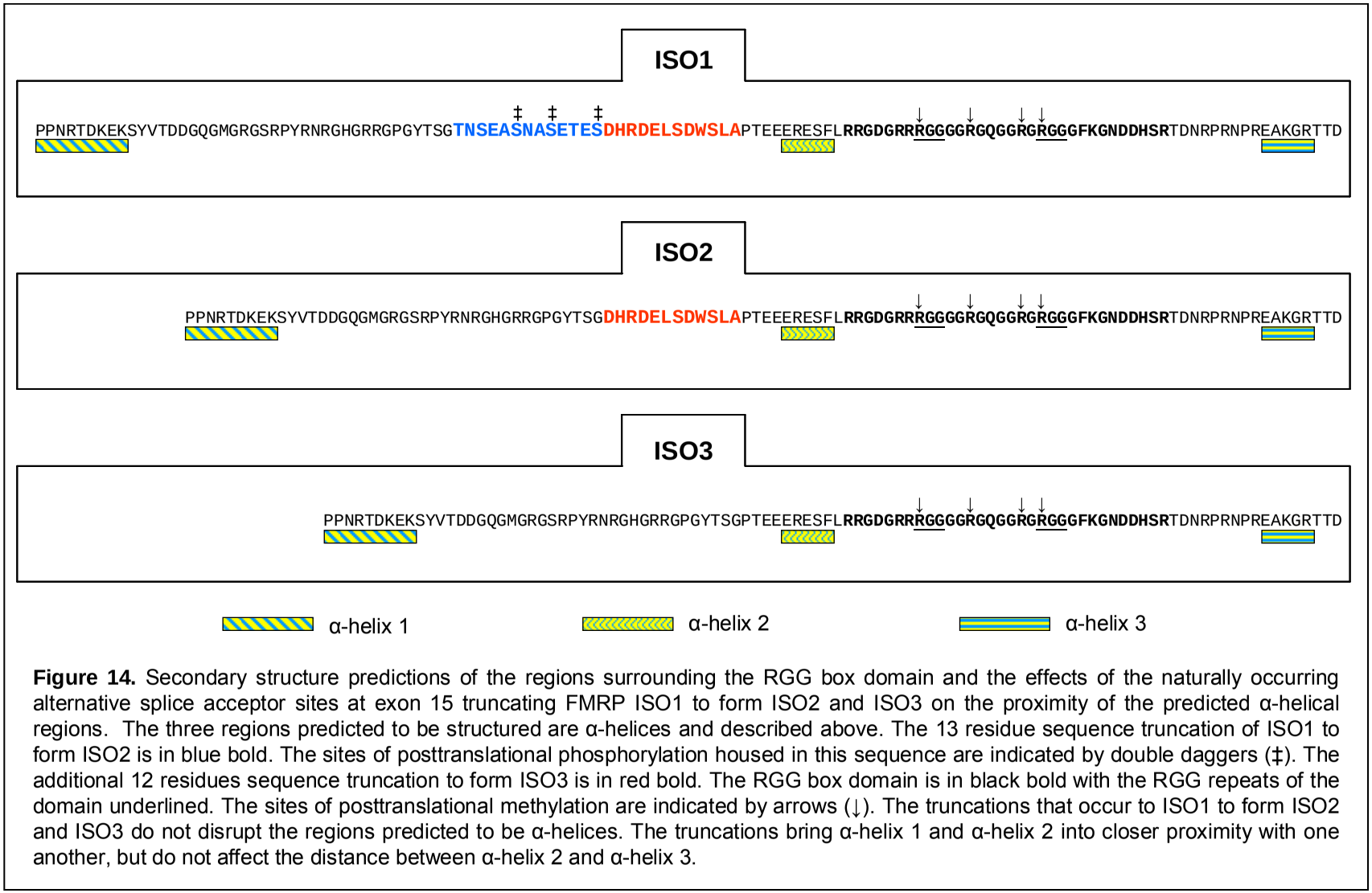

Figure 14. Secondary structure predictions of the regions surrounding the RGG box domain and the effects of the naturally occurring alternative splice acceptor sites at exon 15 truncating FMRP ISO1 to form ISO2 and ISO3 on the proximity of the predicted α-helical regions. The three regions predicted to be structured are α-helices and described above. The 13 residue sequence truncation of ISO1 to form ISO2 is in blue bold. The sites of posttranslational phosphorylation housed in this sequence are indicated by double daggers (‡). The additional 12 residues sequence truncation to form ISO3 is in red bold. The RGG box domain is in black bold with the RGG repeats of the domain underlined. The sites of posttranslational methylation are indicated by arrows (↓). The truncations that occur to ISO1 to form ISO2 and ISO3 do not disrupt the regions predicted to be α-helices. The truncations bring α-helix 1 and α-helix 2 into closer proximity with one another, but do not affect the distance between α-helix 2 and α-helix 3.

predominately unstructured, with a short five residue predicted α-helical sequence (α-helix 2) between two other predicted α-helices (α-helix 1, α-helix 3). The three predicted α-helices are present in all three FMRP isoforms, and it is noteworthy that α-helix 2 is comprised by five of the 10 residues between the sequence eliminated to form ISO3 and the RGG box domain. The distance of the unstructured region between α-helix 2 and α-helix 3 for all three FMRP isoforms is 42 residues, and contains the RGG box domain. The unstructured region between helices 1 and 2 is shortened as ISO1 is truncated to form ISO2, and further again to form ISO3. This separation is 59, 46 or 34 residues, for ISO1, ISO2 or ISO3 respectively, bringing the predicated helix 1 and helix 2 into closer proximity. Additionally, the segments of FMRP truncated when forming ISO2 and ISO3 are predicted to be unstructured. A possible explanation for the increase in binding affinity to G quadruplex mRNA as FMRP is truncated is that the truncations bring helix 1 and helix 2 closer to one another, and as a result helix 3 is also brought closer to helix 1. This would likely cause this region of FMRP to become more structured in general. Considering it is thought that the RGG box domain is unstructured and becomes structured upon binding substrate G quadruplex mRNA, it is possible that increasing the general level of structure for this region containing the RGG box domain will result in the RGG box domain having a better conformation and orientation in space for binding the G quadruplex mRNA to yield a higher probability for a more productive binding event, thus increasing binding affinity as FMRP truncations occur.

The identity of the residues deleted during the alternative splice truncation events could also offer an explanation for the increasingly tighter binding affinity as ISO1 is truncated to form ISO2 and then ISO3 (Figs 5, 13) (Table 2). The sequence deleted to

form ISO2 contains three glutamate residues and no other charged residues, hence giving this 13mer a 3^- overall charge. In addition, the three sites of serine phosphorylation reside in this 13mer, which would increase its negative charge to 9^-. The 12mer deleted to form ISO3 from ISO2 contains three aspartate residues and a glutamate residue, combined for a 4^- charge. However, this 12mer also contains a histidine residue and an arginine residue, resulting in an overall 2^- charge for this 12mer. Combining the 13mer truncated to form ISO2 and the 12mer truncated to form ISO3, the net charge for the overall truncated segment is 5^-. Moreover, if the three serine residues, only present in ISO1, are posttranslationally phosphorylated, the net charge for the overall truncated segment becomes 11^-. Based on the high negative charge character of this region of FMRP, repulsion against the phosphate backbone of the mRNA might occur.

It has been reported that increased FMRP ISO1 binding to FMRP mRNA, containing a guanine-rich sequence in the coding region that potentially forms a G quadruplex structure, decreases the synthesis of FMRP ISO1, and increases the synthesis of FMRP ISO2 and ISO3 [44]. Hence, binding of ISO1, containing the region shown to be posttranslationally phosphorylated, to FMRP mRNA results in the increased synthesis of ISO2 and ISO3, both of which lack the sites of phosphorylation. It is unclear whether the mRNA corresponding to ISO2 and ISO3 are present on the polyribosomes, or if the binding of FMRP ISO1 protein to FMRP ISO1 mRNA triggers an alternative splicing event at the polyribosome followed by translation to form ISO2 and ISO3. Moreover, FMRP ISO3 has been shown to be considerable less methylated on the RGG box domain arginines than ISO1 and ISO2 [41]. Given that FMRP is methylated within its RGG box domain, it stands to reason that this posttranslational modification would reduce its

binding affinity for G quadruplex mRNA. Additionally, our results indicate that FMRP ISO3 has a tighter binding for G quadruplex mRNA than ISO2, which in turn binds tighter than ISO1, when all three isoforms are devoid of posttranslational modifications (Fig 13) (Table 2). Thus, one could envision a model according to which the binding of FMRP ISO1 to FMRP mRNA results in the production of FMRP ISO2 and ISO3, which bind with much higher affinity to other G quadruplex mRNA targets and, at least in the case of ISO3, are resistant to methylation of their RGG box domain arginines, preserving their tight G quadruplex mRNA binding. Therefore, increased binding of ISO1 to FMRP mRNA causes an increase in ISO2 and, more importantly, ISO3 expression, which then enables the cells to increase the tightness in binding and regulating the expression of G quadruplex mRNAs. These events of alternative splicing and posttranslational modifications are clearly mechanisms of FMRP regulation utilized by cells. Further investigation is needed of the individual and combined effects of these events as well as when the cells utilize which events under what cellular conditions and circumstances.

CHAPTER 5: RESULTS AND DISCUSSION – ANALYSIS OF THE TRANSLATION REGULATION ACTIVITY OF FMRP ISOFORMS 1, 2 AND 3 FOR A REPORTER GENE WITH A G QUADRUPLEX STRUCTURE IN THE 5'-UTR

5.1 The Luciferase Reporter Gene Constructs pRM10, pRM11 and pRM12

FMRP has demonstrated mRNA translation regulation activity and binding activity to G quadruplex mRNA [4, 6, 8, 17]. Bioinformatics analysis has revealed that potentially 2334 G quadruplex structures could fold in the 5'-UTR of human mRNA transcripts from known protein-coding genes. Evidence supporting the involvement of G quadruplex mRNA structures in posttranscriptional regulation of gene expression was provided by individually introducing the known G quadruplexes from the 5'-UTRs of two different mRNAs into the mRNA 5'-UTR of a reporter gene and observing that the reporter gene translation was inhibited [25, 26]. Similar results occurred when the proposed G quadruplex forming sequence from the coding region of FMRP mRNA was inserted into the 5'-UTR of a reporter gene [79].

The model developed by Menon et al for FMRP translation regulation proposes that as the local concentration of FMRP relative to G quadruplex mRNA increases, the protein unwinds the G quadruplex structure (Figs 1, 6) [4, 8], allowing for the translation of the target mRNA to occur. To test the ability of the three FMRP isoforms to regulate translation, we have designed a plasmid, pRM10, which contains the G quadruplex sequence from the 5'-UTR of MAP1B mRNA inserted in the 5'-UTR of the firefly luciferase reporter gene (Fig 15). As positive controls, the pRM11 plasmid, with four guanines mutated to cytosine, hence abolishing the G quadruplex structure, and the

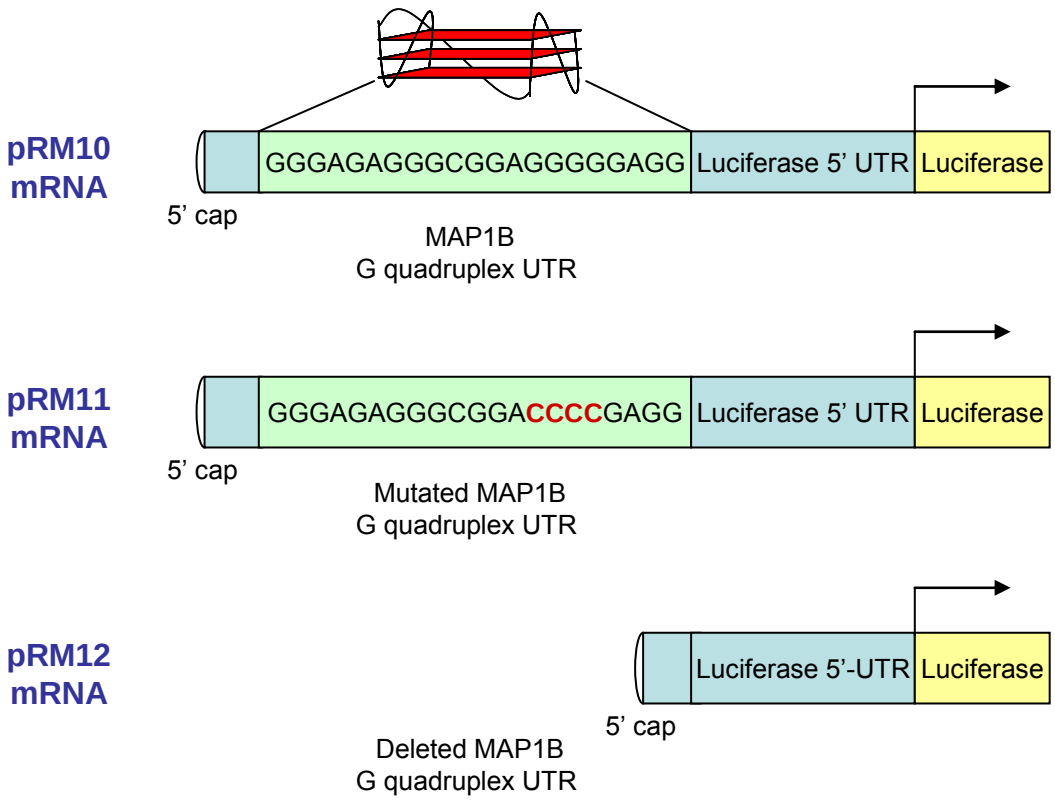

Figure 15. Schematic of the pRM mRNAs utilized, corresponding to their respective plasmids, for the luciferase reporter gene assay to analyze the activity of FMRP to regulate the translation of mRNAs containing the G quadruplex structure and analyze the changes in the FMRP translation regulation activity resulting from the alternative splice truncations. All three pRM mRNAs contain identical sequences from the luciferase mRNA 5'-UTR. The pRM10 mRNA contains in its 5'-UTR the G quadruplex forming sequence from the MAP1B mRNA 5'-UTR. The pRM11 plasmid is identical to pRM10 except four guanine residues (bold red) were mutated to cytosines to abolish the G quadruplex structure. The pRM12 mRNA contains no sequence from the MAP1B mRNA.

pRM12 plasmid, with no included MAP1B mRNA sequence, were designed (Fig 15). All plasmid constructs were confirmed by DNA sequencing. The rationale behind these experiments is that if the proposed model is correct, as more FMRP binds to the MAP1B G quadruplex structure located in the 5'-UTR of the luciferase mRNA, the G quadruplex structure will be unwound, allowing for the translation of the luciferase protein.

5.2 Purification, Restriction Enzyme Digestion and *in vitro* Transcription of pRM10, pRM11 and pRM12 Plasmids

The respective pRM plasmids were purified from BL21 Gold *E. coli* cells, resulting in a typical yield of 150 μg/mL (Fig 16). The purified pRM plasmids were linearized near downstream of the *luc* stop codon via EcoRI restriction enzyme digestion followed by ethanol precipitation purification (Fig 16). The respective linearized pRM plasmids were transcribed *in vitro* to produce the corresponding respective pRM mRNAs (Fig 16). Transcribed pRM mRNAs were purified via ethanol precipitation in preparation for the *in vitro* translation assay to analyze the translation regulation activity of FMRP. The pRM10 mRNA was annealed in the presence of 10 mM K^+ to allow the formation of the G quadruplex structure. The pRM11 and pRM12 mRNAs were similarly annealed although they should not be able to form the G quadruplex structure.

5.3 Analysis of FMRP Translation Regulation Activity for a Reporter Gene Containing a G quadruplex Structure in its mRNA 5'-UTR

It has been previously shown that the presence of a G quadruplex structure in the mRNA 5'-UTR of a reporter gene reduces its translation [26]. Thus, just the presence of the MAP1B G quadruplex structure in the 5'-UTR of the reporter gene mRNA, from pRM10, even in the absence of FMRP ISO1 shows a 95.1% reduction in the luciferase reporter translation relative to the translation of the positive control mRNA from pRM12 (Fig 17, brown bars). As FMRP ISO1 is titrated in at a 1:1 ratio, the *in vitro* translation of pRM10 mRNA is further repressed to 99.8% relative to the translation of the

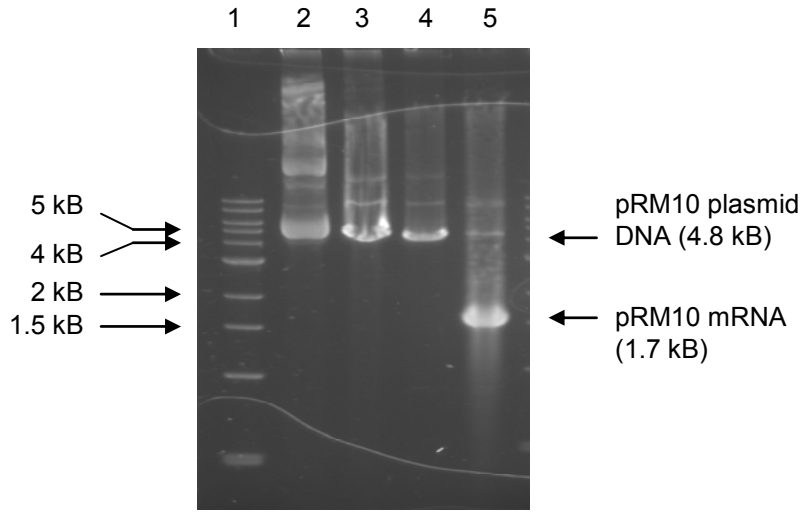

Figure 16. 1% agarose gel electrophoresis analysis of the pRM10 plasmid DNA and *in vitro* transcribed mRNA throughout preparation for the *in vitro* translation reporter gene assay. Lane 1: DNA marker. Lane 2: undigested pRM10 plasmid DNA. Lane 3: EcoRI digested pRM10 plasmid DNA. Lane 4: ethanol precipitated EcoRI digested pRM plasmid DNA. Lane 5: *in vitro* transcribed pRM10 mRNA.

positive control mRNA from pRM12 (Fig 17, red bars). This translation repression is in agreement with the model proposed by Menon et al that when present at low levels, FMRP stabilizes the G quadruplex structure present in the 5'-UTR of the luciferase mRNA (Fig 6) [4]. As the concentration of titrated FMRP ISO1 increases to a 3:1 ratio, the translation of pRM10 mRNA is further repressed to 100% relative to the translation of the positive control mRNA from pRM12 (Fig 17, green bars). Upon titrating FMRP ISO1 to an 8:1 ratio, the pRM10 mRNA translation remains repressed at 100% of the positive control pRM12 mRNA (Fig 17, yellow bars). The luciferase translation results using the pRM10 mRNA are not in full agreement with the proposed model for FMRP translation regulation function (Fig 6). As shown previously using the synthetic RGG box peptide, as the RGG box peptide concentration increases, the G quadruplex structure unwinds [4, 6, 17]. According to the proposed model, as the mRNA G quadruplex

structure unwinds, the mRNA becomes more available for translation. Our *in vitro* translation results support this model when at low levels of FMRP ISO1 (1:1, 3:1), in that the pRM10 translation is repressed (Fig 17). However, at high levels of FMRP ISO1 (8:1), the translation of pRM10 mRNA remains repressed, which does not support the model since the G quadruplex structure was not unwound and translation of pRM10 was not allowed to occur (Fig 17).

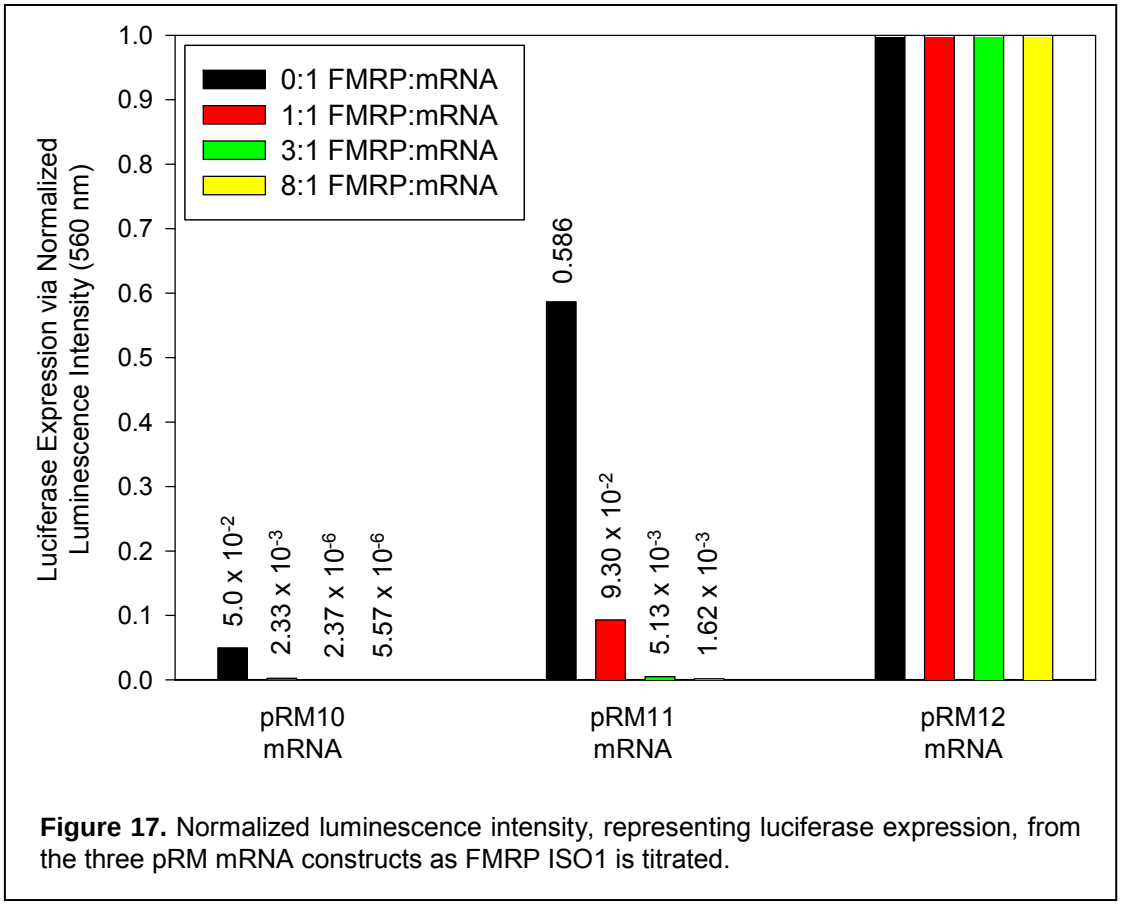

Figure 17. Normalized luminescence intensity, representing luciferase expression, from the three pRM mRNA constructs as FMRP ISO1 is titrated.

The pRM12 reporter gene construct, containing no sequence originating from MAP1B mRNA, has shown to be an effective positive control for luciferase expression since the design of the construct and the presence or absence of FMRP ISO1 has had no

effect on luciferase expression and translation (Figs 15, 17). However, the pRM11 reporter gene construct was not a good negative control. In the absence and presence of FMRP ISO1, we expected the luciferase expression from the pRM11 mRNA to be comparable to that from pRM12, but this was not observed (Figs 15, 17). Analysis of the mutated MAP1B mRNA sequence inserted into the 5'-UTR of the pRM11 construct mRNA indicates that it is possible that the number of guanines mutated to cytosine residues might not have been sufficient to perturb the formation of a G quadruplex structure (Fig 15). Sequence analysis reveals that 12 guanine residues remain from the original MAP1B G quadruplex sequence, and considering that the G quartet structure requires four guanine residues to form a G quadruplex structure, three sets of G quartets stacked could still form a G quadruplex structure in the 5'-UTR of the pRM11 mRNA. It is, however, likely that this G quadruplex structure formed by pRM11 mRNA is different from that of pRM10 mRNA. The potential for pRM11 mRNA to fold into a G quadruplex structure is supported from the 41.4% reduction of luciferase translation, in the absence of FMRP ISO1, relative to the pRM12 mRNA positive control. Further support is provided by the increased translation repression, 90.7%, 99.5%, and 99.8% reduction relative to control, when FMRP ISO1 is titrated to ratios of 1:1, 3:1, and 8:1, respectively, with pRM11 mRNA. The normalization of the luminescence was relative to that for the pRM12 construct for a respective FMRP ISO1 titration point. Additionally, the differences in translation regulation activity between the three FMRP isoforms and determination of the ability of FMRP ISO2 and ISO3 unwind the G quadruplex structure need to be investigated.

CHAPTER 6: CONCLUSIONS

6.1 Expression, Purification and Dialysis of FMRP ISO1, ISO2 and ISO3

The expression protocol of FMRP ISO1, ISO2 and ISO3 was successfully developed and performed using the Rosetta 2(DE3) pLysS *E. coli* cell line. Expression of the FMRP isoforms using *E. coli* is critical in that the expressed proteins are devoid of the posttranslational modifications of phosphorylation and arginine methylation. This enables the analysis of the direct effects of these posttranslational modifications, individually and simultaneously, on the FMRP activity via its RGG box domain for the binding of G quadruplex forming mRNAs as well as other processes in which FMRP has been shown to be involved.

The conditions for the purification of the FMRP isoforms using a single Ni^{2+} affinity chromatography step was developed, reducing the time and processes necessary for purifying the notoriously difficult FMRP. In addition, the protocol for the concentration of the FMRP isoforms was developed, considerably reducing the protein loss from precipitation and membrane adsorption of previous methods.

To prepare the FMRP isoforms for analysis of binding activity for G quadruplex forming mRNAs, the conditions for the dialysis of the FMRP isoforms to remove imidazole were developed. The dialysis protocol developed herein results in the gradual dialysis of the FMRP isoforms and minimizes protein loss through precipitation. Additionally, the dialysis protocol is devoid of K^+ and Na^+ counterions. Various K^+ concentrations are required depending on the G quadruplex mRNA structure that is used

during assays; hence with the FMRP isoforms in a buffer devoid of K^+ enables the addition of a known K^+ concentration as needed.

6.2 Analysis of the Differences in Binding Activity of FMRP ISO1, ISO2 and ISO3 for *in vivo* Neuronal Target G quadruplex Forming mRNA

Differences in the *in vitro* binding activity for *in vivo* neuronal target G quadruplex mRNA between the three longest FMRP isoforms, formed via naturally occurring alternative splicing, was shown from this study. The increase in binding affinity for G quadruplex mRNA as FMRP ISO1 is truncated to form ISO2 and ISO3 was shown herein, further supporting the postulation that alternative splicing serves a mechanism for regulating FMRP activity. However, the rationale, at the molecular level, for how these FMRP truncations result in tighter binding for G quadruplex forming mRNA remains unclear.

6.3 Analysis of the Activity of FMRP ISO1 to Regulate Gene Expression by Regulating Translation

The results do not fully agree with the model proposed by Menon et al for the translation regulation function of FMRP. We have shown that low levels of FMRP repress the translation of an mRNA that contains a G quadruplex structure in its 5'-UTR, which is in agreement with our model. However, as the level of FMRP increases, the level of reporter gene translation is further repressed, in contrast to the proposed model for the mechanism by which FMRP exerts its translation regulation function.

6.4 Future Research

The expression of FMRP ISO1, ISO2 and ISO3 using *E. coli* renders the protein devoid of the posttranslational modifications of serine phosphorylation and arginine methylation. The explicit effects of these modifications, individually and simultaneously, on the binding activity for G quadruplex forming mRNA and translation regulation activity for mRNAs that contain the G quadruplex structure need to be further investigated. To further investigate the effects of alternative splicing on the activity of FMRP, ISO2 and ISO3 need to be applied to the luciferase reporter translation regulation activity assay. In addition, more guanines from the pRM11 construct need to be mutated to assure complete abolishment of the G quadruplex structure for this construct. Recently, a patient diagnosed with the FXS phenotype expressed normal levels of FMRP. Genetic analysis showed that this patient had a guanine insertion that caused a frameshift mutation between the RGG repeats of the RGG box domain, abolishing the second RGG of the repeats, as well as a premature stop codon. The binding activity of this FMRP mutant for G quadruplex forming mRNA and translation regulation activity for mRNAs that contain the G quadruplex structure needs to be further investigated.

REFERENCES

1. Martin, J. B., and Bell, J. (1943) A pedigree of mental defect showing sex-linkage, *J. Neural. Psychiatr. 6*, 157-157.
2. Lubs, H. A. (1969) A marker X chromosome, *American journal of human genetics 21*, 231-244.
3. Crawford, D. C., Acuna, J. M., and Sherman, S. L. (2001) FMR1 and the fragile X syndrome: human genome epidemiology review, *Genet Med 3*, 359-371.
4. Menon, L., Mader, S. A., and Mihailescu, M. R. (2008) Fragile X mental retardation protein interactions with the microtubule associated protein 1B RNA, *RNA (New York, N.Y 14*, 1644-1655.
5. Sofocleous, C., Kolialexi, A., and Mavrou, A. (2009) Molecular diagnosis of Fragile X syndrome, *Expert review of molecular diagnostics 9*, 23-30.
6. Menon, L., and Mihailescu, M. R. (2007) Interactions of the G quartet forming semaphorin 3F RNA with the RGG box domain of the fragile X protein family, *Nucleic acids research 35*, 5379-5392.
7. Jin, P., and Warren, S. T. (2000) Understanding the molecular basis of fragile X syndrome, *Human molecular genetics 9*, 901-908.
8. O'Donnell, W. T., and Warren, S. T. (2002) A decade of molecular studies of fragile X syndrome, *Annual review of neuroscience 25*, 315-338.
9. Siomi, M. C., Higashijima, K., Ishizuka, A., and Siomi, H. (2002) Casein kinase II phosphorylates the fragile X mental retardation protein and modulates its biological properties, *Molecular and cellular biology 22*, 8438-8447.

10. Stetler, A., Winograd, C., Sayegh, J., Cheever, A., Patton, E., Zhang, X., Clarke, S., and Ceman, S. (2006) Identification and characterization of the methyl arginines in the fragile X mental retardation protein Fmrp, *Human molecular genetics 15*, 87-96.

11. Tamanini, F., Bontekoe, C., Bakker, C. E., van Unen, L., Anar, B., Willemsen, R., Yoshida, M., Galjaard, H., Oostra, B. A., and Hoogeveen, A. T. (1999) Different targets for the fragile X-related proteins revealed by their distinct nuclear localizations, *Human molecular genetics 8*, 863-869.

12. Kim, M., Bellini, M., and Ceman, S. (2009) Fragile X mental retardation protein FMRP binds mRNAs in the nucleus, *Molecular and cellular biology 29*, 214-228.

13. Sittler, A., Devys, D., Weber, C., and Mandel, J. L. (1996) Alternative splicing of exon 14 determines nuclear or cytoplasmic localisation of fmr1 protein isoforms, *Human molecular genetics 5*, 95-102.

14. Kiledjian, M., and Dreyfuss, G. (1992) Primary structure and binding activity of the hnRNP U protein: binding RNA through RGG box, *The EMBO journal 11*, 2655-2664.

15. Corley, S. M., and Gready, J. E. (2008) Identification of the RGG box motif in Shadoo: RNA binding and signaling roles?, *Bioinformatics and Biology Insights 2*, 389-406.

16. Zanotti, K. J., Lackey, P. E., Evans, G. L., and Mihailescu, M. R. (2006) Thermodynamics of the fragile X mental retardation protein RGG box interactions with G quartet forming RNA, *Biochemistry 45*, 8319-8330.

17. Bole, M., Menon, L., and Mihailescu, M. R. (2008) Fragile X Mental Retardation Protein Recognition of G quadruplex Structure per se is Sufficient for High Affinity Binding to RNA, *Molecular BioSystems 4*, 1212-1219.

18. Hardin, C. C., Perry, A. G., and White, K. (2000) Thermodynamic and kinetic characterization of the dissociation and assembly of quadruplex nucleic acids, *Biopolymers 56*, 147-194.

19. Valverde, R., Edwards, L., and Regan, L. (2008) Structure and function of KH domains, *The FEBS journal 275*, 2712-2726.

20. Darnell, J. C., Fraser, C. E., Mostovetsky, O., Stefani, G., Jones, T. A., Eddy, S. R., and Darnell, R. B. (2005) Kissing complex RNAs mediate interaction between the Fragile-X mental retardation protein KH2 domain and brain polyribosomes, *Genes & development 19*, 903-918.

21. Chen, A. A., Draper, D. E., and Pappu, R. V. (2009) Molecular simulation studies of monovalent counterion-mediated interactions in a model RNA kissing loop, *Journal of molecular biology 390*, 805-819.

22. Huppert, J. L., Bugaut, A., Kumari, S., and Balasubramanian, S. (2008) G-quadruplexes: the beginning and end of UTRs, *Nucleic acids research 36*, 6260-6268.

23. Simonsson, T. (2001) G-quadruplex DNA structures--variations on a theme, *Biological chemistry 382*, 621-628.

24. Mashima, T., Matsugami, A., Nishikawa, F., Nishikawa, S., and Katahira, M. (2009) Unique quadruplex structure and interaction of an RNA aptamer against bovine prion protein, *Nucleic acids research 37*, 6249-6258.

25. Arora, A., Dutkiewicz, M., Scaria, V., Hariharan, M., Maiti, S., and Kurreck, J. (2008) Inhibition of translation in living eukaryotic cells by an RNA G-quadruplex motif, *RNA (New York, N.Y 14*, 1290-1296.

26. Kumari, S., Bugaut, A., Huppert, J. L., and Balasubramanian, S. (2007) An RNA G-quadruplex in the 5' UTR of the NRAS proto-oncogene modulates translation, *Nature chemical biology 3*, 218-221.

27. Ashley, C. T., Sutcliffe, J. S., Kunst, C. B., Leiner, H. A., Eichler, E. E., Nelson, D. L., and Warren, S. T. (1993) Human and murine FMR-1: alternative splicing and translational initiation downstream of the CGG-repeat, *Nature genetics 4*, 244-251.

28. Devys, D., Lutz, Y., Rouyer, N., Bellocq, J. P., and Mandel, J. L. (1993) The FMR-1 protein is cytoplasmic, most abundant in neurons and appears normal in carriers of a fragile X premutation, *Nature genetics 4*, 335-340.

29. Siomi, H., Siomi, M. C., Nussbaum, R. L., and Dreyfuss, G. (1993) The protein product of the fragile X gene, FMR1, has characteristics of an RNA-binding protein, *Cell 74*, 291-298.

30. Verkerk, A. J. M. H., de Graaf, E., De Boulle, K., Eichler, E. E., Konecki, D. S., Reyners, E., Manca, A., Poustka, A., Willems, P. J., Nelson, D. L., and Oostra, B. (1993) Alternative splicing in the fragile X gene FMR1, *Human molecular genetics 2*, 399-404.

31. Khandjian, E. W., Bechara, E., Davidovic, L., and Bardoni, B. (2005) Fragile X mental retardation protein: many partners and multiple targets for a promiscuous function, *Current Genomics 6*, 515-522.

32. Penagarikano, O., Mulle, J. G., and Warren, S. T. (2007) The pathophysiology of fragile x syndrome, *Annual review of genomics and human genetics 8*, 109-129.

33. Xie, W., Dolzhanskaya, N., LaFauci, G., Dobkin, C., and Denman, R. B. (2009) Tissue and developmental regulation of fragile X mental retardation 1 exon 12 and 15 isoforms, *Neurobiol Dis 35*, 52-62.

34. Cheever, A., and Ceman, S. (2009) Phosphorylation of FMRP inhibits association with Dicer, *RNA (New York, N.Y 15*, 362-366.

35. Ceman, S., O'Donnell, W. T., Reed, M., Patton, S., Pohl, J., and Warren, S. T. (2003) Phosphorylation influences the translation state of FMRP-associated polyribosomes, *Human molecular genetics 12*, 3295-3305.

36. Narayanan, U., Nalavadi, V., Nakamoto, M., Pallas, D. C., Ceman, S., Bassell, G. J., and Warren, S. T. (2007) FMRP phosphorylation reveals an immediate-early signaling pathway triggered by group I mGluR and mediated by PP2A, *J Neurosci 27*, 14349-14357.

37. Narayanan, U., Nalavadi, V., Nakamoto, M., Thomas, G., Ceman, S., Bassell, G. J., and Warren, S. T. (2008) S6K1 phosphorylates and regulates fragile X mental retardation protein (FMRP) with the neuronal protein synthesis-dependent mammalian target of rapamycin (mTOR) signaling cascade, *The Journal of biological chemistry 283*, 18478-18482.

38. Weiler, I. J., Irwin, S. A., Klintsova, A. Y., Spencer, C. M., Brazelton, A. D., Miyashiro, K., Comery, T. A., Patel, B., Eberwine, J., and Greenough, W. T. (1997) Fragile X mental retardation protein is translated near synapses in response

to neurotransmitter activation, *Proceedings of the National Academy of Sciences of the United States of America 94*, 5395-5400.

39. Denman, R. B. (2002) Methylation of the arginine-glycine-rich region in the fragile X mental retardation protein FMRP differentially affects RNA binding, *Cellular & molecular biology letters 7*, 877-883.

40. Dolzhanskaya, N., Merz, G., Aletta, J. M., and Denman, R. B. (2006) Methylation regulates the intracellular protein-protein and protein-RNA interactions of FMRP, *Journal of cell science 119*, 1933-1946.

41. Dolzhanskaya, N., Merz, G., and Denman, R. B. (2006) Alternative splicing modulates protein arginine methyltransferase-dependent methylation of fragile X syndrome mental retardation protein, *Biochemistry 45*, 10385-10393.

42. Ashley, C. T., Jr., Wilkinson, K. D., Reines, D., and Warren, S. T. (1993) FMR1 protein: conserved RNP family domains and selective RNA binding, *Science (New York, N.Y 262*, 563-566.

43. Sung, Y. J., Conti, J., Currie, J. R., Brown, W. T., and Denman, R. B. (2000) RNAs that interact with the fragile X syndrome RNA binding protein FMRP, *Biochemical and biophysical research communications 275*, 973-980.

44. Didiot, M. C., Tian, Z., Schaeffer, C., Subramanian, M., Mandel, J. L., and Moine, H. (2008) The G-quartet containing FMRP binding site in FMR1 mRNA is a potent exonic splicing enhancer, *Nucleic acids research 36*, 4902-4912.

45. Darnell, J. C., Jensen, K. B., Jin, P., Brown, V., Warren, S. T., and Darnell, R. B. (2001) Fragile X mental retardation protein targets G quartet mRNAs important for neuronal function, *Cell 107*, 489-499.

46. Lu, R., Wang, H., Liang, Z., Ku, L., O'Donnell W, T., Li, W., Warren, S. T., and Feng, Y. (2004) The fragile X protein controls microtubule-associated protein 1B translation and microtubule stability in brain neuron development, *Proceedings of the National Academy of Sciences of the United States of America 101*, 15201-15206.

47. Ramos, A., Hollingworth, D., and Pastore, A. (2003) G-quartet-dependent recognition between the FMRP RGG box and RNA, *RNA (New York, N.Y 9*, 1198-1207.

48. Zalfa, F., Giorgi, M., Primerano, B., Moro, A., Di Penta, A., Reis, S., Oostra, B., and Bagni, C. (2003) The fragile X syndrome protein FMRP associates with BC1 RNA and regulates the translation of specific mRNAs at synapses, *Cell 112*, 317-327.

49. Guan, F., Villegas, G., Teichman, J., Mundel, P., and Tufro, A. (2006) Autocrine class 3 semaphorin system regulates slit diaphragm proteins and podocyte survival, *Kidney international 69*, 1564-1569.

50. Nasarre, P., Constantin, B., Rouhaud, L., Harnois, T., Raymond, G., Drabkin, H. A., Bourmeyster, N., and Roche, J. (2003) Semaphorin SEMA3F and VEGF have opposing effects on cell attachment and spreading, *Neoplasia (New York, N.Y 5*, 83-92.

51. Antar, L. N., and Bassell, G. J. (2003) Sunrise at the synapse: the FMRP mRNP shaping the synaptic interface, *Neuron 37*, 555-558.

52. Gabus, C., Mazroui, R., Tremblay, S., Khandjian, E. W., and Darlix, J. L. (2004) The fragile X mental retardation protein has nucleic acid chaperone properties, *Nucleic acids research 32*, 2129-2137.

53. Jin, P., and Warren, S. T. (2003) New insights into fragile X syndrome: from molecules to neurobehaviors, *Trends in biochemical sciences 28*, 152-158.

54. Greenough, W. T., Klintsova, A. Y., Irwin, S. A., Galvez, R., Bates, K. E., and Weiler, I. J. (2001) Synaptic regulation of protein synthesis and the fragile X protein, *Proceedings of the National Academy of Sciences of the United States of America 98*, 7101-7106.

55. Hou, L., Antion, M. D., Hu, D., Spencer, C. M., Paylor, R., and Klann, E. (2006) Dynamic translational and proteasomal regulation of fragile X mental retardation protein controls mGluR-dependent long-term depression, *Neuron 51*, 441-454.

56. Bardoni, B., Schenck, A., and Mandel, J. L. (1999) A novel RNA-binding nuclear protein that interacts with the fragile X mental retardation (FMR1) protein, *Human molecular genetics 8*, 2557-2566.

57. Brown, V., Small, K., Lakkis, L., Feng, Y., Gunter, C., Wilkinson, K. D., and Warren, S. T. (1998) Purified recombinant Fmrp exhibits selective RNA binding as an intrinsic property of the fragile X mental retardation protein, *The Journal of biological chemistry 273*, 15521-15527.

58. Ceman, S., Brown, V., and Warren, S. T. (1999) Isolation of an FMRP-associated messenger ribonucleoprotein particle and identification of nucleolin and the fragile X-related proteins as components of the complex, *Molecular and cellular biology 19*, 7925-7932.

59. Denman, R. B., and Sung, Y. J. (2002) Species-specific and isoform-specific RNA binding of human and mouse fragile X mental retardation proteins, *Biochemical and biophysical research communications 292*, 1063-1069.

60. Laggerbauer, B., Ostareck, D., Keidel, E. M., Ostareck-Lederer, A., and Fischer, U. (2001) Evidence that fragile X mental retardation protein is a negative regulator of translation, *Human molecular genetics 10*, 329-338.

61. Mazroui, R., Huot, M. E., Tremblay, S., Boilard, N., Labelle, Y., and Khandjian, E. W. (2003) Fragile X Mental Retardation protein determinants required for its association with polyribosomal mRNPs, *Human molecular genetics 12*, 3087-3096.

62. Reis, S. A., Willemsen, R., van Unen, L., Hoogeveen, A. T., and Oostra, B. A. (2004) Prospects of TAT-mediated protein therapy for fragile X syndrome, *Journal of molecular histology 35*, 389-395.

63. Sung, Y. J., Dolzhanskaya, N., Nolin, S. L., Brown, T., Currie, J. R., and Denman, R. B. (2003) The fragile X mental retardation protein FMRP binds elongation factor 1A mRNA and negatively regulates its translation in vivo, *The Journal of biological chemistry 278*, 15669-15678.

64. Tamanini, F., Van Unen, L., Bakker, C., Sacchi, N., Galjaard, H., Oostra, B. A., and Hoogeveen, A. T. (1999) Oligomerization properties of fragile-X mental-retardation protein (FMRP) and the fragile-X-related proteins FXR1P and FXR2P, *The Biochemical journal 343 Pt 3*, 517-523.

65. Zhang, Y. Q., Friedman, D. B., Wang, Z., Woodruff, E., 3rd, Pan, L., O'Donnell, J., and Broadie, K. (2005) Protein expression profiling of the drosophila fragile X

mutant brain reveals up-regulation of monoamine synthesis, *Mol Cell Proteomics 4*, 278-290.

66. Degerli, N., and Akpinar, M. A. (2001) A novel concentration method for concentrating solutions of protein extracts based on dialysis techniques, *Analytical biochemistry 297*, 192-194.

67. Valverde, R., Pozdnyakova, I., Kajander, T., Venkatraman, J., and Regan, L. (2007) Fragile X mental retardation syndrome: structure of the KH1-KH2 domains of fragile X mental retardation protein, *Structure 15*, 1090-1098.

68. Gasteiger, E., Gattiker, A., Hoogland, C., Ivanyi, I., Appel, R. D., and Bairoch, A. (2003) ExPASy: The proteomics server for in-depth protein knowledge and analysis, *Nucleic acids research 31*, 3784-3788.

69. Cole, C., Barber, J. D., and Barton, G. J. (2008) The Jpred 3 secondary structure prediction server, *Nucleic acids research 36*, W197-201.

70. Cuff, J. A., and Barton, G. J. (1999) Evaluation and improvement of multiple sequence methods for protein secondary structure prediction, *Proteins 34*, 508-519.

71. Rost, B., Yachdav, G., and Liu, J. (2004) The PredictProtein server, *Nucleic acids research 32*, W321-326.

72. Kneller, D. G., Cohen, F. E., and Langridge, R. (1990) Improvements in protein secondary structure prediction by an enhanced neural network, *Journal of molecular biology 214*, 171-182.

73. Pollastri, G., and McLysaght, A. (2005) Porter: a new, accurate server for protein secondary structure prediction, *Bioinformatics (Oxford, England) 21*, 1719-1720.

74. Zhang, Y., O'Connor, J. P., Siomi, M. C., Srinivasan, S., Dutra, A., Nussbaum, R. L., and Dreyfuss, G. (1995) The fragile X mental retardation syndrome protein interacts with novel homologs FXR1 and FXR2, *The EMBO journal 14*, 5358-5366.

75. Vagenende, V., Yap, M. G., and Trout, B. L. (2009) Mechanisms of protein stabilization and prevention of protein aggregation by glycerol, *Biochemistry 48*, 11084-11096.

76. Shi, R., Pan, Q., Guan, Y., Hua, Z., Huang, Y., Zhao, M., and Li, Y. (2007) Imidazole as a catalyst for in vitro refolding of enhanced green fluorescent protein, *Archives of biochemistry and biophysics 459*, 122-128.

77. Rackham, O., and Brown, C. M. (2004) Visualization of RNA-protein interactions in living cells: FMRP and IMP1 interact on mRNAs, *The EMBO journal 23*, 3346-3355.

78. Bharill, S., Sarkar, P., Ballin, J. D., Gryczynski, I., Wilson, G. M., and Gryczynski, Z. (2008) Fluorescence intensity decays of 2-aminopurine solutions: lifetime distribution approach, *Analytical biochemistry 377*, 141-149.

79. Schaeffer, C., Bardoni, B., Mandel, J. L., Ehresmann, B., Ehresmann, C., and Moine, H. (2001) The fragile X mental retardation protein binds specifically to its mRNA via a purine quartet motif, *The EMBO journal 20*, 4803-4813.